

**FACULTY  
OF MATHEMATICS  
AND PHYSICS**  
Charles University

**MASTER THESIS**

Bc. Michal Matulík

**The role of non-Gaussian entanglement  
of continuous-variable quantum states  
in quantum technologies**

Institute of Particle and Nuclear Physics

Supervisor of the master thesis: Doc. Mgr. Petr Marek, Ph.D.

Study programme: Particle and Nuclear Physics

Study branch: FCJFP

Prague 2023

I declare that I carried out this master thesis independently, and only with the cited sources, literature and other professional sources. It has not been used to obtain another or the same degree.

I understand that my work relates to the rights and obligations under the Act No. 121/2000 Sb., the Copyright Act, as amended, in particular the fact that the Charles University has the right to conclude a license agreement on the use of this work as a school work pursuant to Section 60 subsection 1 of the Copyright Act.

In ..... date .....  
Author's signature

I would like to dedicate this diploma thesis to three special individuals. Firstly, to my supervisor Doc. Mgr. Petr Marek, Ph.D., who gave me the chance to start in the field of quantum optics and information and whose unwavering support, guidance, and mentorship have been crucial to the successful completion of this research. Thank you for your dedication and for believing in me throughout this journey.

Secondly, I would like to express my gratitude to Prof. RNDr. Pavel Cejnar, Dr., Dsc. and Doc. Mgr. Milan Krтіčka, Ph.D., who provided me with the necessary permissions to write this thesis at the Department of Optics at Palacký University. Thank you for making this journey possible.

Title: The role of non-Gaussian entanglement of continuous-variable quantum states in quantum technologies

Author: Bc. Michal Matulík

Institute: Institute of Particle and Nuclear Physics

Supervisor: Doc. Mgr. Petr Marek, Ph.D., Department of Optics, Palacký University, Olomouc

Abstract: We present an effort to find a measure of non-Gaussianity of non-Gaussian states. We compute the difference between the logarithmic negativities of non-Gaussian state and its Gaussified form as a non-Gaussian entanglement resource. We use the latter to assess the resource content of non-Gaussianity of experimentally relevant state - two-mode squeezed vacuum with a subtracted photon. We also used symplectic analysis to discard the Gaussian entanglement. Therefore the measure is reduced to the logarithmic negativity of a non-Gaussian state only. We compare the measure with the Wigner distribution and its negativity and discuss the results.

Keywords: quantum entanglement logarithmic negativity non-Gaussian states measure non-Gaussianity tmsv subtraction photon

# Contents

<b>Introduction</b>	<b>2</b>
<b>1 Methods</b>	<b>4</b>
1.1 Single mode electromagnetic oscillator . . . . .	4
1.2 Quasi-probability distribution . . . . .	6
1.2.1 Wigner representation . . . . .	6
1.2.2 Gaussian and non-Gaussian states . . . . .	8
1.3 Gaussian unitaries . . . . .	8
1.3.1 Vacuum and thermal states . . . . .	9
1.3.2 One-mode squeezing . . . . .	10
1.3.3 Beam splitter . . . . .	11
1.3.4 Two-mode squeezing . . . . .	12
1.4 Bipartite entanglement . . . . .	14
1.4.1 Pure states . . . . .	14
1.4.2 Mixed states . . . . .	15
1.5 Bloch-Messiah decomposition . . . . .	19
1.6 Subtraction of photon . . . . .	20
1.7 Existing measure of non-Gaussianity . . . . .	20
<b>2 Results</b>	<b>22</b>
2.1 Calibration . . . . .	23
2.2 Subtraction of photon . . . . .	25
2.2.1 Looking for measure . . . . .	27
2.3 Comparing to other measures . . . . .	32
2.3.1 Wigner negativity . . . . .	32
<b>Conclusion</b>	<b>35</b>
<b>Bibliography</b>	<b>36</b>
<b>List of Figures</b>	<b>39</b>
<b>List of Abbreviations</b>	<b>40</b>

# Introduction

Quantum information science connects quantum physics with information theory to study the processing, analysis, and transmission of information. Nowadays one of the most promising applications of quantum information is in quantum technologies, especially in quantum computing [1]. It manipulates and processes information. Beyond computing, quantum information is also being used to explore and understand fundamental questions about the nature of reality, such as the role of entanglement in quantum systems. Quantum information comes in two forms, discrete and continuous [2]. For both of these approaches, light is a natural testing ground due to the ease of preparing, manipulating, and measuring suitable quantum states [3].

The continuous-variable (CV) quantum system has an infinite dimensional Hilbert space described by observables with continuous eigenspectra. Such a system is usually a bosonic field, in our case a light field, represented by bosonic modes. All information about the bosonic system is contained in density operator  $\hat{\rho}$ . Any density operator can be represented in terms of quasi-probability distribution - Wigner function. States with a Gaussian Wigner function are Gaussian states and the others are non-Gaussian states. An arbitrary non-Gaussian state can be Gaussified to a Gaussian state due to the same covariance matrix of non-Gaussian and Gaussified states. Unitary operations that transform Gaussian states into Gaussian states are called Gaussian operations [4]. Gaussian states were the first CV states that occurred in quantum technologies due to easy theoretical description [4]. They are also efficiently producible in the laboratory [2, 4]. Regardless of all successes of Gaussian states, they have a major drawback in the context of quantum technologies: all Gaussian measurements of such states can be efficiently simulated [5]. To achieve a quantum computational advantage in the CV, one must consider non-Gaussian states [6, 7]. If one would like to quantify non-Gaussian states in the sense: Given two non-Gaussian states, which one has more non-Gaussianity?, then one finds there is no obvious answer. One of the possibilities is the negative volume of the Wigner function [8]. Is it sufficient or can be non-Gaussian states described by other properties? If yes, which properties should it be? Although there can be found decent development in the area of non-Gaussian states in recent years [8, 9, 10], these questions still remain open.

Another main resource needed in quantum technologies is entanglement. Entanglement is a non-classical correlation between two systems, these correlations cannot be created by any local operations and classical communications [11]. In entanglement theory there are two main questions: Is the state entangled? and if yes, then how much entanglement does it have? A key tool for studying entanglement is a partial transposition (the transposition with respect to one of the two subsystems) [12, 13]. In the case of pure states, the entanglement can be quantified by the entropy of entanglement. For mixed states, there is no single definition of a measure of entanglement [11]. Many of them are not computable. As shown in [14], there is one easy measure to compute, the logarithmic negativity, which can be used both for mixed and pure states. Furthermore, it can be expressed both in terms of the density operator and the covariance matrix [14], which means that it can easily evaluate entanglement of a non-Gaussian state

and its Gaussified form.

In this work, we will analyze a specific example - the subtraction of photons from a two-mode squeezed state (TMSV). The two-mode squeezed state is a Gaussian entangled state that can be prepared, in practice, by parametric amplification, the first realization is in [15]. Photon subtraction that can be realized on a theoretical level by annihilation operators is a non-Gaussian operation. When applied to the two-mode squeezed state, it changes it into a non-Gaussian state and increases its entanglement [16]. In experiments, a generation of non-Gaussian states is challenging, the most recent experiment can be found in [17]. The operation can change both the Gaussian and the non-Gaussian entanglement of the state. However, since the Gaussified state is always an approximation without full information about the state, the non-Gaussian entanglement will be higher than the Gaussian one. The difference between these two kinds of entanglements is therefore an indicator of a non-Gaussian nature of the state. We can now ask a question, whether this difference can be used as a measure for non-Gaussianity, or some different property, of the quantum state.

In the first chapter, we are going to introduce Wigner representation and Gaussian and non-Gaussian states. We present the necessary overview of basic Gaussian unitaries starting with vacuum and thermal states and eventually coming to the TMSV state. The TMSV is the first instance of quantum entanglement in continuous variable systems. After that the logarithmic negativity as a measure of entanglement in mixed states is introduced. The first chapter is ended with a basic tool of a symplectic analysis - Bloch-Messiah decomposition. In the second chapter, we have tried to derive a non-Gaussianity measure denoted as  $\Delta$ . We used TMSV with one subtracted photon in superposition denoted as  $|\psi\rangle$ . We discuss why is  $\Delta$  good measure and we try to interpret the measure with the help of the Wigner negativity.

# 1. Methods

We present an overview of needed tools and methods. The quantization of the electromagnetic field is not presented in the following text, straight away we start with the quantized light field. We use

$$\hbar = 1$$

notation throughout the thesis.

## 1.1 Single mode electromagnetic oscillator

The quantization of an electromagnetic field leads to  $N$  pairs of bosonic operators corresponding to  $N$  quantized modes, i.e.  $N$  quantum harmonic oscillators. Hilbert space of these  $N$  bosonic modes is a tensor product of Hilbert spaces of individual modes  $\mathcal{H} = \otimes_{k=1}^N \mathcal{H}_k$ . Hilbert space  $\mathcal{H}$  is infinitely large and separable. A consequence of the tensor product is the possibility to find out how each pair of mode operators, in particular annihilation and creation operator, determines an individual Hilbert space [18]. We will usually work within one mode and then we try to generalize some results into multi modes.

A pair of bosonic operators must satisfy the Bose commutation relation

$$[\hat{a}, \hat{a}^\dagger] = 1. \quad (1.1)$$

The single-mode Hilbert space is spanned by countable basis  $\{|n\rangle\}_0^\infty$  called Fock basis (or number-state basis). These basis states are eigenstates of a number operator  $\hat{n}$ :

$$\hat{n} = \hat{a}^\dagger \hat{a}, \quad \hat{n}|n\rangle = n|n\rangle. \quad (1.2)$$

The bosonic operators  $\hat{a}$  and  $\hat{a}^\dagger$ , annihilation and creation operators respectively, lowers and raises photon number in integer steps

$$\hat{a}|n\rangle = \sqrt{n}|n-1\rangle, \quad \hat{a}^\dagger|n\rangle = \sqrt{n+1}|n+1\rangle. \quad (1.3)$$

There is one more additional condition to the annihilation operator

$$\hat{a}|0\rangle = 0, \quad (1.4)$$

where  $|0\rangle$  is the lowest (ground) state. Intuitively, we cannot find any lower state that is the ground state. Note, the mode operators of different modes commute, naturally, they represent distinct physical systems.

We can also describe the bosonic system by other field operators. These are the quadrature operators  $\hat{q}$  and  $\hat{p}$ . They can be interpreted as a real and an imaginary part of the complex amplitude<sup>1</sup>  $\hat{a}$

$$\hat{q} = \frac{1}{\sqrt{2}}(\hat{a}^\dagger + \hat{a}), \quad \hat{p} = \frac{i}{\sqrt{2}}(\hat{a}^\dagger - \hat{a}). \quad (1.5)$$

---

<sup>1</sup>Note that in Eq.1.5 we could use a different definition, e.g.  $\hat{q} = (\hat{a}^\dagger + \hat{a})$ .



Inverse relations are

$$\hat{a} = \frac{1}{\sqrt{2}}(\hat{q} + i\hat{p}), \quad \hat{a}^\dagger = \frac{1}{\sqrt{2}}(\hat{q} - i\hat{p}). \quad (1.6)$$

From Eq.1.1 we can see that they satisfy

$$[\hat{q}, \hat{p}] = i. \quad (1.7)$$

We can easily generalize Bose commutation relation 1.1 to  $N$ -mode case using a formal vector  $\hat{\mathbf{b}} = (\hat{a}_1, \hat{a}_1^\dagger, \dots, \hat{a}_N, \hat{a}_N^\dagger)^T$ , which must also satisfy [4]

$$[\hat{b}_i, \hat{b}_j] = i\Omega_{ij},$$

where  $\Omega$  is block-diagonal  $2N \times 2N$  matrix with diagonal matrices  $J$

$$\Omega = \bigoplus_1^N J = \begin{pmatrix} J & & \\ & \ddots & \\ & & J \end{pmatrix}, \quad J = \begin{pmatrix} 0 & 1 \\ -1 & 0 \end{pmatrix}. \quad (1.8)$$

We can also arrange pairs of  $\{\hat{q}_k \hat{p}_k\}_{k=1}^N$  into the formal vector

$$\hat{\mathbf{x}} = (\hat{q}_1, \hat{p}_1, \dots, \hat{q}_N, \hat{p}_N)^T. \quad (1.9)$$

So we can reformulate one-mode commutation relation 1.7 to the multi-mode case

$$[\hat{x}_i, \hat{x}_j] = i\Omega_{ij}. \quad (1.10)$$

It is not a coincidence that we used  $q$  and  $p$  symbols. The commutation relation 1.7 is the same as for quantization of the position and momentum of the harmonic oscillator. The quantization of the electromagnetic field leads to an analogy of the quantization of the harmonic oscillator and quadratures  $\hat{q}$  and  $\hat{p}$  can be regarded as position and momentum respectively. It is easily seen from the Hamiltonian of the quantized electromagnetic field with unit frequency [18]

$$\hat{H} = \hat{n} + \frac{1}{2} = \frac{\hat{q}^2}{2} + \frac{\hat{p}^2}{2}. \quad (1.11)$$

A single mode of the quantized electromagnetic field is equivalent to an oscillator with position  $\hat{q}$  and momentum  $\hat{p}$ , so-called the electromagnetic oscillator.

The quadrature states are eigenstates of  $\hat{q}$  and  $\hat{p}$

$$\hat{q}|q\rangle = q|q\rangle, \quad \hat{p}|p\rangle = p|p\rangle. \quad (1.12)$$

Their spectrum is continuous. They are orthogonal and complete therefore create bases  $\{|q\rangle\}_{q \in \mathbb{R}}$ ,  $\{|p\rangle\}_{p \in \mathbb{R}}$ . We can pass from one basis to another by Fourier transform because  $\hat{q}$  and  $\hat{p}$  obey canonical commutation relation

$$|p\rangle = \frac{1}{\sqrt{2\pi}} \int \exp(iqp)|q\rangle dq,$$

$$|q\rangle = \frac{1}{\sqrt{2\pi}} \int \exp(-iqp)|p\rangle dp.$$

We are also able to generalize it to the multi-modes

$$\hat{\mathbf{x}}^T |\mathbf{x}\rangle = \mathbf{x}^T |\mathbf{x}\rangle. \quad (1.14)$$

Note that  $\mathbf{x}$  are continuous variables. We have come to a definition of a continuous-variable system: a quantum system is called a continuous-variable system when it has an infinite-dimensional Hilbert space described by observables with continuous eigenspectra [4]. The quadrature states are useful to define quadrature wave functions  $\psi(q) = \langle q|\psi\rangle$  and  $\psi(p) = \langle p|\psi\rangle$  as well.

## 1.2 Quasi-probability distribution

In classical mechanics, we can represent a state of a system as a point in phase space  $(p, q)$ , where  $p$  and  $q$  are canonical variables. If we want to describe statistical properties of classical systems e.g. classical oscillator, we can come up with a probability distribution function  $W(q, p)$ , then this distribution quantifies the probability of finding pair of  $q$  and  $p$  values in simultaneous measurements. If statistical distribution is known, we can calculate all statistical quantities, so we have a full description of a given state. In the hope of the successful introduction of density matrix as a complete description of quantum systems, we can look for a quantum analog of a probability distribution  $W(q, p)$ . It turns out that  $W(q, p)$  can be negative. Therefore we talk about quasi-probability distribution  $W(q, p)$  [18, 19]. We will often refer to the Wigner distribution as the Wigner function.

### 1.2.1 Wigner representation

Let us briefly sketch the derivation of the Wigner distribution, The Wigner function can be obtained by postulating its properties [18]. We assume that the distribution behaves like a joint probability distribution of  $q$  and  $p$ , therefore the marginals of the distribution must give the position and momentum probability distributions. To connect it with quantum mechanics we postulate

$$\langle q|\hat{\rho}|q\rangle = \int W(q, p)dp, \quad (1.15a)$$

$$\langle p|\hat{\rho}|p\rangle = \int W(q, p)dq. \quad (1.15b)$$

The left-hand sides also generate probability distribution but in the whole Hilbert space, where  $\hat{\rho}$  is defined. We have connected quasi-probability distribution  $W(q, p)$  to quantum mechanics. Notice, these formulas also connect quantum states to observations. This can be used in quantum tomography to measure marginals and thus reconstruct the quantum state [18].

If we want to find an explicit form of  $W(q, p)$ , we define a characteristic function  $\chi(u, v)$ . It is Fourier transformation of  $W(q, p)$ :

$$\chi(u, v) = \int W(q, p) \exp(iuq - ivp)dqdp. \quad (1.16)$$

Actually, we can look at the characteristic function as an expectation value [19]

$$\chi(u, v) = \langle \exp(iuq - ivp) \rangle_W \quad (1.17)$$

A quantum analog of the expectation value for arbitrary  $\hat{\rho}$  is

$$C(u, v) = \text{tr}(\hat{\rho} \exp(iu\hat{q} - iv\hat{p})), \quad (1.18)$$

where the introduced operator

$$\hat{D}(u, v) = \exp(iu\hat{q} - iv\hat{p}) \quad (1.19)$$

is the Weyl operator. So  $C(u, v)$  is a "quantum Fourier transform" of density operator. We came up to

$$C(u, v) = \chi(u, v).$$

After the classical inverted Fourier transform, we get the Wigner quasi-probability distribution

$$W(x, p) = \int \frac{1}{(2\pi)^2} \exp(-i(uq - vp)) C(u, v) du dv. \quad (1.20)$$

Let us explicitly calculate the trace in Eq.1.18 and then the characteristic function  $C(u, v)$ . The Baker-Husdorff formula is as useful as the appropriate substitution  $q \rightarrow x + v/2$  in the last step of

$$\begin{aligned} C(u, v) &= \int \langle q | \hat{\rho} \exp(iu\hat{q} - iv\hat{p}) | q \rangle dq \\ &= \exp(-i\frac{uv}{2}) \int \exp(iuq) \langle q | \hat{\rho} | q - v \rangle dq \\ &= \int \exp(iux) \langle x + \frac{v}{2} | \hat{\rho} | x - \frac{v}{2} \rangle dx. \end{aligned} \quad (1.21)$$

According to Eq.1.20, the Wigner function can be extract from  $C(u, v)$  by inverted Fourier transform

$$W(q, p) = \frac{1}{2\pi} \int \exp(ipv) \langle q + \frac{v}{2} | \hat{\rho} | q - \frac{v}{2} \rangle dv, \quad (1.22)$$

where we used the traditional formula for the Delta function

$$\delta(x - q) = \frac{1}{2\pi} \int \exp(iu(x - q)) du.$$

The Wigner function from the momentum representation can be obtained in a similar way.

As usual, we would like to generalize the Wigner function 1.22 to the multi-mode case. Instead of  $q$  and  $p$ , we use the same  $2N$ -dimensional vector  $\mathbf{x}$  as in the section above. Therefore, we introduce a  $2N$ -dimensional vector  $\boldsymbol{\xi}$  in the same units as  $u$  and  $v$ . The Weyl operator is then

$$\hat{D}(\boldsymbol{\xi}) = \exp(i\hat{\mathbf{x}}^T \Omega \boldsymbol{\xi}), \quad (1.23)$$

The characteristic function has a similar form as in the one-mode case

$$C(\boldsymbol{\xi}) = \text{tr}(\hat{\rho} \hat{D}(\boldsymbol{\xi})). \quad (1.24)$$

Finally, the general Wigner function is

$$W(\mathbf{x}) = \int \frac{d^{2N} \boldsymbol{\xi}}{(2\pi)^{2N}} \exp(-i\mathbf{x}^T \Omega \boldsymbol{\xi}) C(\boldsymbol{\xi}). \quad (1.25)$$

Therefore, continuous variables  $\mathbf{x}$  span a real  $\mathbb{R}^{2N}$  space called phase space.

Let us introduce a few basic properties for the one-mode case,  $N = 1$ . It is real  $W(q, p) = W^*(q, p)$ , for Hermitian  $\hat{\rho}$ . It can be easily verified from Eq.1.22. The Wigner function is normalized

$$\int W(q, p) dq dp = 1 \quad (1.26)$$

because of normalization  $\text{tr}(\hat{\rho}) = 1$ . For us, the most important property of the Wigner function is its negativity, more in Sec.1.7.

## 1.2.2 Gaussian and non-Gaussian states

We have introduced the phase space representation of the continuous variable quantum states. We can distinguish two types of states occurring in the Wigner representation: Gaussian and non-Gaussian states [4, 10]. Gaussian states are easy to characterize. By definition, their Wigner function is a Gaussian

$$W(\mathbf{x}) = \left( (2\pi)^N \sqrt{\det V} \right)^{-1} \exp \left( -\frac{1}{2} (\mathbf{x} - \bar{\mathbf{x}})^T V^{-1} (\mathbf{x} - \bar{\mathbf{x}}) \right). \quad (1.27)$$

Mean values are arranged in the similar formal vector  $\bar{\mathbf{x}} = \langle \hat{\mathbf{x}} \rangle = \text{tr}(\hat{\mathbf{x}}\hat{\rho})$  as the vector of the quadratures and the vector of their eigenvalues  $\hat{\mathbf{x}}$  and  $\mathbf{x}$ , respectively. The second moments are arranged into the covariance matrix  $V$  whose elements are defined by

$$V_{ij} = \frac{1}{2} \langle \{ \Delta \hat{x}_i, \Delta \hat{x}_j \} \rangle, \quad (1.28)$$

where  $\Delta \hat{x}_i = \hat{x}_i - \langle \hat{x}_i \rangle$  and the curly brackets represent the anti-commutator. The last equality defines the covariance matrix for any quantum state. If we set the first moment to zero<sup>2</sup> in Gaussian state 1.27 then its Wigner function is completely characterized by the covariance matrix  $V$ . The covariance matrix is real and symmetric. It has a  $2N \times 2N$  form. It must satisfy the uncertainty principle [20]

$$V + \frac{i}{2} \Omega \geq 0. \quad (1.29)$$

This matrix equation means that the matrix sum on the left-hand side has only non-negative eigenvalues. Eq.1.29 is a direct consequence of the commutation relation 1.10 and of the non-negativity of  $\hat{\rho}$ .<sup>3</sup> Eq.1.29 implies  $V > 0$ . Note that Eq.1.29 applies to any state, not only the Gaussian state.

Contrary to nicely described Gaussian states there is a vast and wild set of non-Gaussian states. All states with non-Gaussian Wigner functions are contained within this class. If we compare pure Gaussian and pure non-Gaussian states then the pure state can have a positive Wigner function if and only if the state is Gaussian [21]. This no longer holds for mixed states. There are states, which are non-Gaussian but have positive Wigner function, examples can be found in [10]. Therefore, if one wants to create a characterization of non-Gaussian states based only on the negative volume of the Wigner function, he or she will quickly be limited by that fact above.

## 1.3 Gaussian unitaries

We have to start with the Gaussian states before the non-Gaussian come to the scene because the non-Gaussian states are usually created from the Gaussian. First of all we introduce transformation  $T$ , which takes quantum state  $\hat{\rho}$  into  $T(\hat{\rho})$ ,

<sup>2</sup>Without loss of generality the first moments can be set to zero with the usage of local unitary displacement operators [30].

<sup>3</sup>If we consider an operator matrix  $\hat{\mathbf{x}}\hat{\mathbf{x}}^T$ , it can be written in terms of anti-commutator and commutator of its factors, then from the definition of expectation value  $\langle \hat{\mathbf{x}}\hat{\mathbf{x}}^T \rangle = \text{tr}(\hat{\mathbf{x}}\hat{\mathbf{x}}^T\hat{\rho})$  we know that  $\langle \hat{\mathbf{x}}\hat{\mathbf{x}}^T \rangle \geq 0$ , due to positive definiteness of  $\hat{\rho}$ . From the anti-commutator, we get the definition of  $V$  and that is all we need to show the necessity of the relation 1.29.

it is called a quantum operation. The simplest case is for the trace-preserving and reversible transformations, quantum channels, they are represented by unitary transformations  $U^\dagger = U^{-1}$  [4], for which  $T(\hat{\rho}) = U\hat{\rho}U^\dagger$ .<sup>4</sup> Gaussian operation is a quantum operation which preserves the Gaussian character of the state, in other words, they always transform a Gaussian state into a Gaussian state. Gaussian unitaries (channels) are generated via  $U = \exp(-i\hat{H}/2)$  from Hamiltonians which are second-order polynomials in the field operators [2, 4]. A Gaussian unitary can be reformulated into a language of quadrature operators ( $\equiv$  transition to the Heisenberg picture). Gaussian unitary corresponds to the transformation of quadrature operators. There exists a whole group of transformations that act on the quadratures. It is called the symplectic group  $\text{Sp}(4, R)$ . It is a set of linear transformations  $S$  of a four-dimensional vector space over the  $R$ . It preserves commutation relation 1.10:

$$\begin{aligned} S \in \text{Sp}(4, R) : \quad & S\Omega S^T = \Omega, \\ \hat{\mathbf{x}} \rightarrow \hat{\mathbf{x}}' = S\hat{\mathbf{x}}, \quad & [\hat{x}'_i, \hat{x}'_j] = i\Omega_{ij}. \end{aligned} \quad (1.30)$$

Clearly, eigenvalues  $\mathbf{x}$  of the quadrature  $\hat{\mathbf{x}}$  have to follow the same map  $\mathbf{x} \rightarrow \mathbf{x}' = S\mathbf{x}$ . Thus an arbitrary Gaussian unitary in the Hilbert space is equivalent to a symplectic map acting on the phase space. As a consequence of the action of  $S$  on the phase space, the Wigner function is transformed  $W(\mathbf{x}) \rightarrow W(S^{-1}\mathbf{x})$  while the covariance matrix is transformed by  $V \rightarrow SVS^T$ , it can be seen from the definition of the Wigner function.

In the following, we are going to introduce one- and two-mode squeezed states, their appropriate unitaries, and beam splitter transformation. For a more complete overview of different Gaussian unitaries and states the reader may take a look into e.g.: [4].

### 1.3.1 Vacuum and thermal states

Definitely, the most important Gaussian state is the vacuum (ground) state,  $|0\rangle$ . The wave function of the vacuum state can be obtained from Eq.1.4 if we use  $\hat{p} = -i\partial/\partial q$  in the  $q$  representation

$$\psi_0(q) = \pi^{-1/4} \exp\left(-\frac{q^2}{2}\right). \quad (1.31)$$

Even if the light mode is empty, we have to associate a physically meaningful state with this vacuum. If we measured quadrature fluctuations of the vacuum, we would get a Gaussian distribution [18]. This can be seen from the covariance matrix. For the vacuum state, the covariance matrix is diagonal  $V = \frac{1}{2}I$ , where  $I$  is the  $2 \times 2$  identity matrix, which means that position and momentum operators have the same variances  $V(\hat{q}) = V(\hat{p}) = \frac{1}{2}$ . From Eq.1.29 we see that the variances fulfill the Heisenberg uncertainty principle

$$V(\hat{q})V(\hat{p}) \geq \frac{1}{4}. \quad (1.32)$$

Thermal states are defined as

$$\hat{\rho}^{th} = \frac{e^{-\beta\hat{H}}}{\text{tr}(e^{-\beta\hat{H}})}. \quad (1.33)$$

---

<sup>4</sup>Bare in mind, we do not use hats over the unitaries throughout the thesis.

The reason why it is called the thermal state can be found in statistical physics, the probability of obtaining an eigenenergy  $E_n$  of the Hamiltonian  $\hat{H}$  is

$$P(E_n) = \langle E_n | \hat{\rho}^{th} | E_n \rangle = \frac{e^{-\beta E_n}}{Z}, \quad (1.34)$$

where  $Z$  is the partition function, but this is exactly the probability distribution of states (probability for finding a certain  $E_n$  for a system at temperature  $T$ ) that maximizes the entropy. The system has maximum entropy at thermodynamic equilibrium. The thermal states are maximizing the entropy. For the electromagnetic oscillator of the light mode, the partition function  $Z$  can be summed up, therefore the mean number of photons  $\bar{n} \equiv \langle n \rangle$  is the famous Bose-Einstein distribution. If we consider that the non-diagonal elements of the Boltzmann distribution 1.34 are zero and for the harmonic oscillator the eigenstates of  $\hat{H}$  are Fock states we can reformulate the density matrix into

$$\hat{\rho}^{th}(\bar{n}) = \sum_{n=0}^{\infty} \frac{e^{-\beta E_n}}{Z} |n\rangle \langle n| = \sum_{n=0}^{\infty} \frac{\bar{n}^n}{(1 + \bar{n})^{1+n}} |n\rangle \langle n|.$$

It is a Gaussian state with zero mean and the covariance matrix  $V = (\bar{n} + \frac{1}{2})I$ .

### 1.3.2 One-mode squeezing

So far, we have met states that were balanced in their variances of the quadratures (the coherent states were skipped we will not need them in what follows). Therefore a natural question arises: What are the minimum uncertainty states? The Heisenberg uncertainty principle of Eq.1.32 gives us that variances of the quadratures should hold that equation, but we can excess the variance in one quadrature and shrink in the other one. Let us parameterize the variances of quadratures with a squeezing parameter  $r$

$$V(\hat{q}) = \frac{1}{2}e^{-2r}, \quad V(\hat{p}) = \frac{1}{2}e^{2r}. \quad (1.35)$$

Obviously, the product of the variances equals the minimal value of 1/4. The wave function of the squeezed vacuum is equivalent to the wave function of vacuum Eq.1.31 with scaled position and different normalization factor

$$\phi(q) = e^{-r/2} \psi_0(e^{-r} q). \quad (1.36)$$

The wave function in the momentum representation has  $+r$  in the exponent. The corresponding Gaussian unitary is the one-mode squeezing operator, which is defined as

$$\hat{U}_{Sq}(r) = \exp\left(\frac{r}{2}(\hat{a}^2 - \hat{a}^{\dagger 2})\right) = \exp\left(i\frac{r}{2}(\hat{x}\hat{p} + \hat{p}\hat{x})\right). \quad (1.37)$$

Squeezed vacuum state is then  $|\phi\rangle = \hat{U}_{Sq}(r)|0\rangle$ . In the Heisenberg picture, the quadrature operators  $\hat{\mathbf{x}} = (\hat{q}, \hat{p})^T$  are transformed by the symplectic map  $\hat{\mathbf{x}} \rightarrow S_{Sq}(r)\hat{\mathbf{x}}$ , where

$$S_{Sq}(r) = \begin{pmatrix} e^{-r} & 0 \\ 0 & e^r \end{pmatrix} \quad (1.38)$$

as can be seen from Eq.1.36.

An experimental realization of the single-mode squeezed states provided proof of the quantum theory of light [22] forty years ago.

The photon statistics of the coherent state is Poissonian distribution [18]. The photon statistics of the squeezed vacuum state are rather different

$$p_n = |\langle n | \hat{U}_S | 0 \rangle|^2.$$

After simple calculations, it turns out that  $p_n$  is zero for odd photon states. A squeezed vacuum contains only photon pairs. It can be explained thanks to the form of Gaussian unitary 1.37.

The Gaussian unitary can be viewed as a unitary evolution of a given Hamiltonian. Consequently, we know the form of the quadratic Hamiltonian. This Hamiltonian is responsible for the specific physical process that generates the squeezed vacuum state. This process is known as parametric down conversion. The beam of laser light, which is focused on a non-linear crystal, induces electric dipoles in the atoms of that crystal. The atoms oscillate with that beam frequency and emit electromagnetic radiation - light. The law of energy conservation is valid, so the energy of the incoming photons must add up to the energy of the emitted photons. The non-trivial case is a pair production [18], where the crystal emits pairs of signal photons, and the incoming beam is called the pumping beam. This process can be used in parametric amplifier. In a degenerate parametric amplifier a signal at the frequency  $\omega$  is amplified by pumping a crystal at frequency  $2\omega$ . Usually, a simple model of a degenerate parametric amplifier is considered where the pump at  $2\omega$  is classical and the signal mode at  $\omega$  is described by the annihilation operator [23]. The such process corresponds to one-mode squeezing 1.37.

### 1.3.3 Beam splitter

To extend squeezing into two modes, we have to introduce a beam splitter. An ideal beam splitter is a reversible device and a lossless device in which two incident beams may interfere to produce two outgoing beams [18]. If we send back the two outgoing beams without changing their phase we reconstruct the original beam. Theoretically, it is modeled as a four-port device with two input and two output beams. The incident fields are described by the annihilation operators  $\hat{a}_1$  and  $\hat{a}_2$  and the outgoing beams are characterized by the  $\hat{a}'_1$  and  $\hat{a}'_2$ . Thus, we are looking for a transformation matrix  $B$  of the Bogoliubov transformation  $(\hat{a}'_1, \hat{a}'_2)^T = B(\hat{a}_1, \hat{a}_2)^T$ . Elements of the matrix  $B$  are  $t$  and  $v$ , transmissivity and reflectivity respectively

$$B = \begin{pmatrix} t & -v \\ v & t \end{pmatrix}. \quad (1.39)$$

The elements  $t$  and  $v$  can be defined through parameter  $\Theta$ ,  $t = \cos(\Theta/2)$  and  $v = \sin(\Theta/2)$ , therefore the relation  $t^2 + v^2 = 1$  accounts for the energy conservation. The matrix  $B$  represents a rotation of the amplitude operators. The symplectic map  $\hat{\mathbf{x}} \rightarrow S_B(\tau)\hat{\mathbf{x}}$  can be deduced from the Bogoliubov transformation of Eq.1.39

$$S_B(\tau) = \begin{pmatrix} tI & -vI \\ vI & tI \end{pmatrix}, \quad (1.40)$$

where  $I$  is an  $2 \times 2$  identity matrix and  $\hat{\mathbf{x}} = (\hat{q}_1, \hat{p}_1, \hat{q}_2, \hat{p}_2)$ .

To find a Gaussian unitary of the beam splitter, we have to switch to the Schrödinger picture. We would like to find unitary operator  $\hat{U}_B$  that evolve state  $|\psi\rangle$  as  $|\psi'\rangle = \hat{U}_B|\psi\rangle$ . It turns out [18] that  $\hat{U}_B$  is given by

$$\hat{U}_B = \exp\left(i\frac{\theta}{2}(\hat{x}_1\hat{p}_2 - \hat{p}_1\hat{x}_2)\right). \quad (1.41)$$

The parameter  $\Theta$  determines the transmissivity of the beam splitter. The beam splitter is balanced if parameter  $\theta = \frac{\pi}{2}$ . If we use formalism of the quadrature wave functions  $\psi(q_1, q_2)$ , we get from Eq.1.41 transformed wave function  $\psi'(q_1, q_2) = \psi(q'_1, q'_2)$ . We know that eigenvalues of the quadratures  $\hat{q}_i$  are in the position representation just  $q_i$ , so they are transformed by matrix  $B$ , eventually the wave function

$$\psi'(q_1, q_2) = \psi(tq_1 + vq_2, -vq_1 + tq_2), \quad (1.42)$$

is simply rotated.

### 1.3.4 Two-mode squeezing

Two-mode squeezing involves two modes of the electromagnetic field which exhibit quantum noise reduction below the noise of the ground state. Two-mode squeezed vacuum can be produced from the interference of two oppositely squeezed vacuum states

$$\phi_1(q_1) = \frac{e^{r/2}}{\sqrt[4]{\pi}} \exp\left(-\frac{1}{2}e^{2r}q_1^2\right), \quad (1.43a)$$

$$\phi_2(q_2) = \frac{e^{-r/2}}{\sqrt[4]{\pi}} \exp\left(-\frac{1}{2}e^{-2r}q_2^2\right), \quad (1.43b)$$

at the balanced beam splitter ( $\tau = \rho = 1/\sqrt{2}$ ).

$$\phi'(q_1, q_2) = \frac{1}{\sqrt{\pi}} \exp\left(-\frac{1}{4}e^{2r}(q_1 + q_2)^2 - \frac{1}{4}e^{-2r}(q_1 - q_2)^2\right). \quad (1.44)$$

In the momentum representation state  $\phi'(p_1, p_2)$  is similar

$$\phi'(p_1, p_2) = \frac{1}{\sqrt{\pi}} \exp\left(-\frac{1}{4}e^{2r}(p_1 - p_2)^2 - \frac{1}{4}e^{-2r}(p_1 + p_2)^2\right). \quad (1.45)$$

In the next, we argue why is the two-mode squeezed vacuum viewed as the EPR state [24]. First of all, let us remind you about the EPR paradox: Einstein, Podolsky, and Rosen considered two spatially separated particles that show a maximum correlation between their positions and their momenta. A measurement of the position of the first particle implies with certainty the position of the second particle and a measurement of the momentum of the second particle implies with certainty the momentum of the first particle. This thought experiment (Gedankenexperiment) led Einstein, Podolsky, and Rosen to the conclusion, that quantum mechanics is not complete, because in quantum mechanics we cannot know the position and momentum of one object simultaneously. Later, Schrödinger came up with the term *Entanglement* [25].

Two-mode squeezing is often seen as the EPR state in its original formulation in terms of continuous position and momentum observables, hence it is the first



instance of continuous-variable entanglement because the wave functions 1.44 and 1.45 describe an entangled state due to quadratures which are correlated. For strong squeezing  $r \rightarrow \infty$  the wave function 1.44 nearly vanishes unless  $q_1 = q_2$  and the wave function 1.45 vanishes unless  $p_1 = -p_2$ . The first possibility of observing the EPR correlations was introduced in [26].

Let us introduce the corresponding quantum state of light to the wave function of Eq.1.44: [18]

$$|\text{TMSV}\rangle \equiv |\psi\rangle = \hat{U}_{S12}|0,0\rangle, \quad (1.46)$$

where  $\hat{U}_{S12}$  is a two-mode squeezing operator

$$\hat{U}_{S12} = \exp\left(-r(\hat{a}_1\hat{a}_2 - \hat{a}_1^\dagger\hat{a}_2^\dagger)\right) = \exp\left(-ir(\hat{x}_1\hat{p}_2 + \hat{p}_1\hat{x}_2)\right). \quad (1.47)$$

Please note, that the squeezing parameter  $r$  is real. We will not need a symplectic map of quadratures, but let us briefly comment on it. The symplectic map is in the form of hyperbolic rotation, or Lorentz transformation

$$S_{Sq2} = \begin{pmatrix} I \cosh r & Z \sinh r \\ Z \sinh r & I \cosh r \end{pmatrix},$$

thus amounts to a re-scaling along the rotated axis and inverse re-scaling along the other. This is equivalent to two one-mode squeezing operators and a beam splitter, as shown in the wave function formalism.  $Z$  is  $2 \times 2$  diagonal matrix with  $Z = \text{diag}(1,-1)$ .

Not just the correlations of the quadratures are expected but also the correlations of two photons are expected. Since both photons have been in their vacuum states after pair production each photon in mode one must be accompanied by a partner in mode two [18]. It is possible to rewrite 1.46 in the Fock representation as

$$|\text{TMSV}\rangle = \sqrt{1 - \lambda^2} \sum_{n=0}^{\infty} \lambda^n |n, n\rangle, \quad (1.48)$$

where  $\lambda(r) = \tanh(r)$ . A proof is simple, we will show that 1.47 and 1.48 obey the same first-order differential equation [18]

$$\begin{aligned} (\hat{a}_1^\dagger\hat{a}_2^\dagger - \hat{a}_1\hat{a}_2)|\psi\rangle &= (\hat{a}_1^\dagger\hat{a}_2^\dagger - \hat{a}_1\hat{a}_2) \sum_{n=0}^{\infty} \frac{(\tanh r)^n}{\cosh r} |n, n\rangle \\ &= \sum_{n=0}^{\infty} \frac{(\tanh r)^n}{\cosh r} \left( (n+1)|n+1, n+1\rangle - n|n-1, n-1\rangle \right) \\ &= \sum_{n'=0}^{\infty} \frac{(\tanh r)^{n'-1}}{\cosh r} \left( n' - (n'+1)(\tanh r)^2 \right) |n', n'\rangle \\ &= \frac{\partial}{\partial r} \sum_{n'=0}^{\infty} \frac{(\tanh r)^{n'}}{\cosh r} |n', n'\rangle = \frac{\partial}{\partial r} |\psi\rangle, \end{aligned} \quad (1.49)$$

in the third step we use proper substitutions ( $n \rightarrow n' \pm 1$ ) and in the fourth we know  $(\tanh r)' = 1 - (\tanh r)^2$ .

The two-mode squeezed states were experimentally observed a few years after the observation of single-mode states [15].

Similarly as in the case of one-mode squeezing, from the Gaussian unitary, we can see the physical process of generating a two-mode squeezed vacuum. The non-degenerate parametric amplifier is a simple generalization of the degenerate parametric amplifier considered in the previous section. Instead of one mode at one signal frequency, we have to consider two modes with frequencies  $\omega_1$  and  $\omega_2$ . The law of energy conservation still holds,  $2\omega = \omega_1 + \omega_2$ . Usually, photons in one outgoing mode are called signals and the others are called idlers. Thus the system is described by two different annihilation operators. This corresponds to the two-mode squeezing 1.47.

Optical parametric amplifiers are widely used everywhere where entangled photons are needed, e.g. in quantum teleportation [27], in Bell tests [28], or even in the production of single photon states [29].

## 1.4 Bipartite entanglement

In Section 1.3.4 we have discovered a coincidence between quadrature measurements and the EPR state. After the discovery of entanglement, a natural question arises whether we can find a measure of entanglement. If someone would like to quantify entanglement, the first thing they need is a criterion of separability. It is also important to distinguish between pure and mixed states because measures of entanglement are not the same for both types of states.

### 1.4.1 Pure states

To begin with, consider two Hilbert space  $\mathcal{H} = \mathcal{H}_A \otimes \mathcal{H}_B$ . It corresponds to a global bipartite system. Imagine a system described by state  $|\Psi\rangle$ , we are allowed to write the system in the form

$$|\Psi\rangle = \sum_{i,j} c_{ij} |e_A^i\rangle \otimes |e_B^j\rangle, \quad (1.50)$$

where  $\{|e_A^i\rangle \otimes |e_B^j\rangle\}$  is an orthonormal product basis. The system is separable if  $|\Psi\rangle$  can be described as a product of states of individual subsystems

$$|\Psi\rangle = |\psi\rangle_1 \otimes |\psi\rangle_2. \quad (1.51)$$

Otherwise  $|\Psi\rangle$  is called entangled.

An introduction of quantum entropy is motivated by information and thermodynamic entropies.<sup>5</sup>

$$S(\hat{\rho}) = -\text{tr}(\hat{\rho} \ln \hat{\rho}) = -\sum_i \rho_i \ln \rho_i, \quad \hat{\rho} = \sum_i \rho_i |i\rangle\langle i|. \quad (1.52)$$

---

<sup>5</sup>Let us have a set of random variables  $i$  with a given probability  $p_i$ , Shannon (information) entropy  $H$  measures the average amount of information content conveyed by knowing outcome  $i$  of random trial:  $H = -\sum_i p_i \ln p_i$ ,  $\sum_i p_i = 1$ . Less probability  $p_i$  of event  $i$  gives more entropy  $H$ . If  $p_i = 0$  or  $= 1$  then  $H = 0$ , so there is no information we can get. In thermodynamics, there is the Gibbs entropy:  $S = -k_B \sum_i p_i \ln p_i$ . It is a measure of all possible microstates in equilibrium compatible with a given macrostate. We can understand  $S$  in the context of  $H$ : Entropy of the macrostate is a measure of how much information is 'missing' to know which microstate occurs.

$S(\hat{\rho})$  can be understood as a measure of 'mixedness' of  $\hat{\rho}$ . This can be used to quantify the entanglement of a pure bipartite system. Let us explain: If the system is entangled then its subsystems are in mixed states (after partial tracing [19]) and vice versa if the system is separable then its subsystems are in pure states. So we can use 1.52 to measure the mixedness of a state of either one or the other subsystem. The more mixed the subsystems are, the more entanglement is in the whole system. Please note it does not depend on the selected subsystem because every state of a coupled system can be expressed in a Schmidt form

$$|\Psi\rangle = \sum_n c_n |\chi_{1n}, \chi_{2n}\rangle,$$

where  $c_n$  is Schmidt number. Consequently, reduced density operators  $\hat{\rho}_i$  of  $\hat{\rho} = |\Psi\rangle\langle\Psi|$  have same diagonal form with elements  $|c_n|^2$ . Note, if system is separable, then  $|c_n|^2 = 0$  or  $|c_n|^2 = 1$ . Finally, the entropy of the subsystems is

$$S(\hat{\rho}_i) = -\sum_n c_n^2 \ln c_n^2 = -\text{tr}(\hat{\rho}_i \ln \hat{\rho}_i).$$

Later we will discuss why we did not choose entropy as the measure of the entanglement even if the TMSV is a pure state.

## 1.4.2 Mixed states

In the beginning, we will show formulas usually for the two-mode states, they are the simplest bipartite systems. Eventually, we will come to expressions that are valid in multi-mode bipartite systems.

### Peres-Horodecki criterion

Consider again two Hilbert space  $\mathcal{H} = \mathcal{H}_A \otimes \mathcal{H}_B$  of a global bipartite system. The motivation why the mixed states are important can be found in real-world experiments, it is an environment where mixed states usually emerge. Then we are forced to use density matrix formalism  $\hat{\rho}$  instead of  $|\Psi\rangle$ . The separability of a mixed state is no longer equivalent to product states, as in the case of pure states. One calls the mixed state of the bipartite system separable if it can be written as a convex combination of product states

$$\hat{\rho} = \sum_i p_i \hat{\rho}_i^A \otimes \hat{\rho}_i^B, \quad (1.53)$$

where  $p_i \geq 0$  and  $\sum_i p_i = 1$ ,  $\hat{\rho}_i^A$  and  $\hat{\rho}_i^B$  are defined on local Hilbert spaces  $\mathcal{H}_A$  and  $\mathcal{H}_B$ . The problem is that we cannot use the same separability condition as in the case of a pure bipartite system. The first practical criterion of separability was introduced by Peres and Horodecki [12, 13], it is called the positive partial transpose criterion (PPT) and it employs the properties of partial transposition. It is the transposition with respect to one of the two subsystems, usually denoted with an index  $T_i$ ,  $i = A, B$ . In fact, if a quantum state  $\hat{\rho}$  is separable then the new density matrix, e.g.  $\hat{\rho}^{T_B}$  is a density operator, i.e., it has a non-negative spectrum, thus it is a quantum state. In a language of matrix elements of  $\hat{\rho}^{T_B}$  the partial transposition of separable state  $\hat{\rho}$  is

$$\langle k, l | \hat{\rho}^{T_B} | k', l' \rangle \equiv \langle k, l' | \hat{\rho} | k', l \rangle.$$

Therefore, the positivity of the partial transposition is a necessary condition for a separable state. On the other hand, the non-positivity of a single negative eigenvalue of the partially transposed density operator is a sufficient condition for an entangled state.

The PPT can be seen in terms of maps. The PPT demands the positivity of the operator  $(I_A \otimes T_B)(\hat{\rho})$ , where  $T_B$  is a transposition map. Transposition is a positive operation, but it is not completely positive.<sup>6</sup> As a consequence, partial transpose is a non-physical operation that can change an entangled quantum state into a non-physical one.

Let us extend the PPT criterion into continuous-variable states. Noting that density matrix  $\hat{\rho}$  is a Hermitian operator, then transposition corresponds to complex conjugation. For the time evolution of a quantum system described by the Schrödinger equation, complex conjugation is equivalent to time reversal. Hence, intuitively, the transposition of a density operator means time reversal. In the continuous variables, it corresponds to a sign change of the momentum variables [30]

$$\hat{\rho} \rightarrow \hat{\rho}^T \Leftrightarrow W(q, p) \rightarrow W(q, -p). \quad (1.54)$$

Also, it can be seen from the definition of the Wigner function 1.22. The two-mode states are the simplest of continuous-variable bipartite systems. From that follows the partial transposition of the density operator of the bipartite system of two modes transforms the Wigner function as

$$W(q_1, p_1, q_2, p_2) \rightarrow W(q_1, p_1, q_2, -p_2). \quad (1.55)$$

This corresponds to a mirror reflection or local time reversal

$$\mathbf{x} \rightarrow \Lambda \mathbf{x}, \quad \Lambda = \text{diag}(1, 1, 1, -1), \quad (1.56)$$

where  $\mathbf{x} = (q_1, p_1, q_2, p_2)$  is a formal four-vector. This general transposition rule is in the case of two-mode Gaussian states of Eq.1.27 reduced to the transformation of the covariance matrix

$$V \rightarrow \tilde{V} = \Lambda V \Lambda \quad (1.57)$$

Since transformed  $W(q_1, p_1, q_2, -p_2)$  is also a Wigner function if the state is separable, from Eq.1.29 we have

$$\tilde{V} + \frac{i}{2}\Omega \geq 0. \quad (1.58)$$

The matrix  $\Omega$  is based on its definition 1.8, it has  $4 \times 4$  block diagonal form. The equation 1.58 is a necessary condition for the separability of two-mode bipartite Gaussian states. Notice, Eq.1.57 and Eq.1.58 hold also for any multi-mode bipartite Gaussian states.

We can simplify the condition 1.58, for that, we use a basic tool in symplectic analysis - Williamson's theorem [31] (sometimes called symplectic decomposition) which gives the possibility of carrying out the symplectic diagonalization of real

---

<sup>6</sup>An operator is positive *iff* it is Hermitian and has non-negative eigenvalues.

A positive map maps any positive operator into a positive one.

The map  $T$  is completely positive *iff*  $I \otimes T$  is positive for identity map  $I$  on any finite dimensional system.

matrices in even dimensions under the definite positivity constraint

$$V = SV^\oplus S^T, \quad V^\oplus = \begin{pmatrix} \nu_- & & & \\ & \nu_- & & \\ & & \nu_+ & \\ & & & \nu_+ \end{pmatrix}. \quad (1.59)$$

The diagonal elements  $\nu_\pm$  are called the symplectic eigenvalues and  $\nu_- \leq \nu_+$ . The diagonal matrix  $V^\oplus$  is called the Williamson form of  $V$ . The matrix  $S$  is the symplectic matrix as defined in Sec.1.3. Please note, it can be generalized into  $N$ -modes

$$V^\oplus = \bigoplus_{k=1}^N \nu_k I, \quad (1.60)$$

where  $I$  is  $2 \times 2$  unit matrix. The symplectic spectrum can be computed as the standard eigenspectrum of the matrix  $|i\Omega V|$ , where the modulus must be understood in the operational sense.

Let us go back to the PPT criterion. We can use the power of the symplectic spectrum to express the fundamental properties of the state, specifically the separability of the state. So the arbitrary  $V$  is a quantum covariance matrix if and only if it satisfies  $V > 0$  and  $\nu_- \geq 1/2$ . A truth of this statement can be seen from uncertainty principle 1.29 which implies  $SVS^T > 0$  because we already know that uncertainty principle gives  $V > 0$  and from the eigenvalues of  $i\Omega/2$ . If the state is separable, then  $\tilde{V}$  also satisfies uncertainty principle 1.58 as discussed. Since  $\tilde{V} > 0$ , this is equivalent to check  $\tilde{\nu}_- \geq 1/2$ , where  $\tilde{\nu}_-$  is the minimal eigenvalue of the symplectic spectrum of  $\tilde{V}$ . That is the separability criterion.

Due to general Eq.1.60 the separability criterion holds for any multi-mode bipartite Gaussian state.

We could continue in modification of the criterion, e.g. with symplectic invariants but it is not necessary [30, 32, 34]. Instead, we introduce analytical expression for symplectic eigenvalues  $\nu_\pm$  and  $\tilde{\nu}_\pm$ .

The two-mode Gaussian states are special because we can find exact analytical expressions for  $\nu_\pm$  and  $\tilde{\nu}_\pm$ . The covariance matrix  $V$  of the two-mode Gaussian state can be expressed in the following block form

$$V = \begin{pmatrix} A & C \\ C^T & B \end{pmatrix}, \quad (1.61)$$

$A, B, C$  are  $2 \times 2$  real matrices. It can be seen from the definition of the covariance matrix 1.28. Then the symplectic spectrum  $\nu_\pm$  is given

$$\nu_\pm = \sqrt{\frac{\Delta \pm \sqrt{\Delta^2 - 4\det V}}{2}}, \quad (1.62)$$

where  $\Delta = \det A + \det B + 2\det C$  and  $\det$  is determinant [32, 33]. For  $\tilde{\nu}_\pm$  we just change a sign in  $\Delta = \det A + \det B - 2\det C$ .

### Logarithmic negativity

For mixed states, we do not have a single definition of measure of entanglement [11]. There are many ways how to get different entanglement measures [11]. Our

focus will be on an axiomatic approach because we will get easily computable measures. In short, any function can be an entanglement measure if it satisfies certain postulates [11]. The most important of them is monotonicity under local operations and classical communication (LOCC).<sup>7</sup> The entanglement cannot increase under LOCC. For any LOCC operation  $\Lambda$  and the entanglement measure  $E(\hat{\rho})$  the postulate above is written as

$$E(\Lambda(\hat{\rho})) \leq E(\hat{\rho}). \quad (1.63)$$

If a function  $E$  satisfies the monotonicity axiom, it means that  $E$  should be constant on separable states, because every separable state can be converted by LOCC to any other separable state [11]. It is reasonable to set this constant to zero. Naturally, we can invert this condition to the basic axiom: every entanglement should disappear on separable states. Those two axioms impose  $E$  to be non-negative. We can also think of other axioms, we can require normalization of  $E$ , so on maximally entangled states, it counts  $e$ -bits.

An easy measure to calculate is so-called logarithmic negativity [14]. It is a direct consequence of the PPT criterion. To understand logarithmic negativity it is better to start with negativity

$$\mathcal{N}(\hat{\rho}) = \sum_{\lambda < 0} \lambda, \quad (1.64)$$

where  $\lambda$  are eigenvalues of  $\hat{\rho}^{T_B}$  (partially transposed density matrix with respect to  $B$ -part of the bipartite system). It quantifies how much the state fails to satisfy the positivity of the partial transpose condition. It vanishes for unentangled states. It can be proved that  $\mathcal{N}$  does not increase under LOCC and it is an entanglement monotone [14]. Another version of the measure is logarithmic negativity given by

$$E_{\mathcal{N}}(\hat{\rho}) = \log_2 \|\hat{\rho}^{T_B}\|_1, \quad (1.65)$$

where  $\|\hat{A}\|_1 = \text{tr}(\sqrt{\hat{A}\hat{A}^\dagger})$  is a trace norm of the Hermitian operator  $\hat{A}$ , which is equal to the sum of the absolute values of the eigenvalues of  $\hat{A}$ . If  $\|\hat{\rho}^{T_B}\|_1 = 1$  then  $E_{\mathcal{N}} = 0$ . The logarithmic negativity is an additive quantity. It can be seen from the identity  $\|\hat{\rho}_1 \otimes \hat{\rho}_2\|_1 = \|\hat{\rho}_1\|_1 \|\hat{\rho}_2\|_1$  (it is best shown from the definition of the trace norm via eigenvalues) and from the additive properties of the logarithm  $E_{\mathcal{N}}(\hat{\rho}_1 \otimes \hat{\rho}_2) = E_{\mathcal{N}}(\hat{\rho}_1) + E_{\mathcal{N}}(\hat{\rho}_2)$ . Both quantities  $\mathcal{N}$  and  $E_{\mathcal{N}}$  are practically computable as we will see.

As in the previous subsection, we have to exactly formulate the logarithmic negativity 1.65 for bipartite Gaussian states. This was done in [14]. If the state is not separable, the uncertainty principle 1.58 does not hold, and  $\tilde{V}$  may fail to be the positive operator. However, we have introduced symplectic diagonalization 1.60 of  $\tilde{V}$ , then  $\tilde{V}$  is equal to the tensor product of the operators with symplectic eigenvalues on diagonal 1.60. The trace norm of this tensor product, as shown above, is just the product of the trace norms. We can modify the definition of

---

<sup>7</sup>Local quantum operation is performed on part of the system, and the result is communicated classically to another part. We have tried to introduce quantum operations in Sec.1.3, but a much wider definition can be found in [11]. Thus a proper definition of LOCC can be also found in [11].

the logarithmic negativity 1.65 for  $N$ -mode bipartite Gaussian states as follows

$$E_{\mathcal{N}}(\hat{\rho}) = \sum_k^N F(\tilde{\nu}_{k=1}), \quad (1.66)$$

where  $F(\tilde{\nu}) = \log_2 \|\hat{\rho}_{\nu}\|_1$  and  $\hat{\rho}_{\nu}$  is the operator whose Wigner function is a Gaussian. It can be shown [14], that  $F(\nu)$  vanishes for  $\nu \geq 1/2$  and for  $\nu < 1/2$  is  $F(\nu) = -\log_2(2\nu)$ .

We stress once more that for Gaussian states Eq.1.65 is equal to Eq.1.66. For non-Gaussian states, this does not hold.

## 1.5 Bloch-Messiah decomposition

The need for this subsection will become apparent in the computation section. We have already started with a symplectic analysis namely the symplectic eigenvalues were useful for the computation of the logarithmic negativity. At the beginning of Gaussian unitaries in Sec.1.3 we have stated that for every Gaussian  $U_S$  in Hilbert space, there exists  $S$  in the phase space. The symplectic decomposition of Eq.1.60 corresponds to the thermal decomposition because we know that thermal states 1.3.1 have diagonal covariance matrix with a diagonal element equal to  $\bar{n} + 1/2$ , in our case the diagonal element of  $V^{\oplus}$  is  $\nu_k$ , therefore  $\bar{n} = \nu_k - 1/2$ . For  $S$  in 1.60 there exists  $U_S$  such that

$$\hat{\rho}(V) = U_S \hat{\rho}(V^{\oplus}) U_S^{\dagger}, \quad (1.67)$$

where

$$\hat{\rho}(V^{\oplus}) = \bigotimes_{k=1}^N \hat{\rho}^{th}(\nu_k - \frac{1}{2}) \quad (1.68)$$

is a tensor product of one-mode thermal states. There is another decomposition.

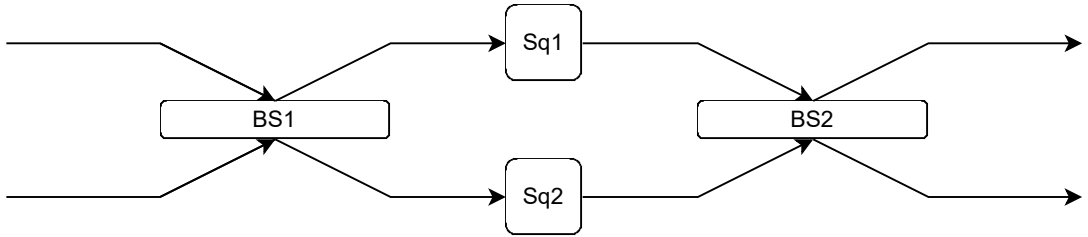


Figure 1.1: Bloch-Messiah decomposition

The canonical unitary  $U_S$  can be decomposed using the Bloch-Messiah decomposition [35]

$$U_S = U_{B2} \left[ \bigotimes_{k=1}^N U_{Sq}(r_k) \right] U_{B1}, \quad (1.69)$$

where  $[\bigotimes_{k=1}^N U_{Sq}(r_k)]$  is a set of  $N$  one-mode squeezers sandwiched between beam splitters  $U_{Bi}$ . If we combine the thermal decomposition of Eq.1.67 with the Bloch-Messiah decomposition of Eq.1.69, then an arbitrary multi-mode Gaussian state  $\hat{\rho}(V)$  can be realized by preparing  $N$  thermal states  $\hat{\rho}(V^{\oplus})$ , applying multi-mode

interferometers and one-mode squeezer. The Bloch-Messiah decomposition can be expressed in terms of symplectic matrices, particularly

$$S = S_{B2} \left[ \bigoplus_{k=1}^N S_{S_q}(r_k) \right] S_{B1}. \quad (1.70)$$

Eq.1.70 will be useful in numerical calculations. We remind you that we will be interested in the two-mode states then we set  $N = 2$ . Previously, we have denoted  $\nu_{\pm} \equiv \nu_{1,2}$ .

Please note, our case is not the most general one because we have considered the first statistical moment equal to zero. In the opposite case, we should have included a displacement operator to Eq.1.67.

## 1.6 Subtraction of photon

Here comes the section, where we will finally generate non-Gaussian states. From a theoretical point of view, a generation of non-Gaussian states is not too different from Gaussian states. It suffices to apply non-Gaussian unitary transformations that would allow for the deterministic generation of non-Gaussian states as in the case of presented Gaussian states. From an experimental point of view is this approach hard to obtain. Thus another approach is conditional. It is based on a different experimental approach, where one measures part of the system and conditions on a certain measurement outcome. On a theoretical level, it is done by the action of a combination of quadrature operators on a system [10]. The most simple case is single-photon subtraction or addition. For single photon subtraction the annihilation  $\hat{a}$  is used on the system  $\hat{\rho}$ ,

$$\hat{\rho} \rightarrow \frac{\hat{a}\hat{\rho}\hat{a}^\dagger}{\text{tr}(\hat{a}\hat{\rho}\hat{a}^\dagger)}. \quad (1.71)$$

The experiment setup consists of a high transmissivity beam splitter, it splits some light of the incident field toward a photodetector. Click on this photodetector represents one subtracted photon, thus this corresponds to conditional preparedness of subtracted state [36]. The most recent experiment in multi-photon subtraction can be found in, e.g. [17].

## 1.7 Existing measure of non-Gaussianity

We have created non-Gaussian states in the previous section, now we would like to know if there exists some measure of non-Gaussianity. Obviously, one can think of negative values of the Wigner function, so-called Wigner negativity. There is one natural measure of the Wigner negativity [37]. We are looking for a measure, which has to be zero if and only if the Wigner function is Gaussian. The starting point is the normalization of the Wigner function 1.26. It implies

$$\int_{\mathbb{R}^{2N}} d\mathbf{x} |W(\mathbf{x})| \geq 1,$$



where  $N$  is the number of modes. That equality is always strict when the Wigner function is non-negative. The easiest measure of the Wigner negativity is through the negative volume [37]

$$W_{\mathcal{N}}(\hat{\rho}) = \int_{\mathbb{R}^{2N}} d\mathbf{x} |W(\mathbf{x})| - 1. \quad (1.72)$$

By definition, the quantity  $W_{\mathcal{N}}(\hat{\rho})$  is equal to zero for coherent and squeezed states, for which  $W$  is non-negative. Similarly, as in the case of entanglement negativity and logarithmic negativity, there was recently introduced Wigner logarithmic negativity (WLN) [8]

$$W_{\mathcal{LN}}(\hat{\rho}) = \log \left( \int_{\mathbb{R}^{2N}} d\mathbf{x} |W(\mathbf{x})| \right).$$

Notice that the WLN is computable in the sense that its value can usually be assessed by numerical integration.

We will use the Wigner negativity in a discussion of numerical results in the next chapter.

## 2. Results

Our ultimate goal is to find a new measure of non-Gaussianity based on the existing entanglement measure, the logarithmic negativity. First of all, we need a Gaussian entangled state, the simplest entangled state in the CV is the TMSV Sec.1.3.4

$$|\text{TMSV}\rangle = \sqrt{1 - \lambda^2} \sum_{n=0}^{\infty} \lambda^n |n, n\rangle, \quad (2.1)$$

corresponding density operator is  $\hat{\rho}_{\text{TMSV}} = |\text{TMSV}\rangle\langle\text{TMSV}|$ . To obtain a non-Gaussian state, it is appropriate to subtract a photon from the Gaussian state as discussed in Sec.1.6. Single photon subtracted states are theoretically obtained by acting with an annihilation operator on the state. Subtraction of a photon is given by

$$|\psi\rangle = M \sum \lambda^n (c_1 \hat{a}_1 + c_2 \hat{a}_2) |n, n\rangle, \quad (2.2)$$

$M$  is a normalization constant and corresponding density operator is  $\hat{\rho} = |\psi\rangle\langle\psi|$ . The annihilation operators always act on one mode of the Hilbert space, i.e.  $\hat{a}_1 = (\hat{a} \otimes I)$  and  $\hat{a}_2 = (I \otimes \hat{a})$ . The normalization constant  $M$  can be easily computed as

$$M = \frac{1 - \lambda^2}{\lambda}. \quad (2.3)$$

The coefficients  $c_1$  and  $c_2$  fulfill a condition

$$c_1^2 + c_2^2 = 1, \quad c_1, c_2 \in \mathbb{R}. \quad (2.4)$$

Thus  $c_i$  can be represented by one parameter  $\theta$ . We set

$$c_1 = \cos \theta, \quad c_2 = \sin \theta. \quad (2.5)$$

In this way, we have obtained a dose of non-Gaussian states parameterized by squeezing parameter  $\lambda$  and subtraction  $\theta$ .

We would like to extract a clear non-Gaussian entanglement from the given non-Gaussian state  $|\psi\rangle$ . To do that, we need to compute the logarithmic negativity of the non-Gaussian state and its Gaussified form.

The logarithmic negativity of a general bipartite state  $\hat{\rho}_\chi$  can be computed directly from the definition 1.65, we will denote the logarithmic negativity computed in this way by the symbol  $E_{\mathcal{N}_{NG}}$ . Let us briefly remind you of the definition: The logarithmic negativity  $E_{\mathcal{N}_{NG}}$  is calculated as a sum of the absolute values of the eigenvalues of the partially transposed  $\hat{\rho}_\chi$ . To numerically compute the  $E_{\mathcal{N}_{NG}}$ , we chose programming language - *Python* with external library *QuTip* [38]. In the *QuTip* environment, we can easily program an arbitrary state based on truncated Fock space, the dimension of the Fock space  $N$  has to be finite. Thus the  $E_{\mathcal{N}_{NG}}$  of the state is just an approximation because it depends on the chosen dimension of the state

$$E_{\mathcal{N}_{NG}} \rightarrow E_{\mathcal{N}_{NG}}(N), \quad N = \dim \text{ of trunc. Fock space.}$$

The logarithmic negativity of a general bipartite Gaussian state  $\hat{\rho}_{\chi G}$  can be computed from the determination of the covariance matrix  $\tilde{V}$ , where  $\tilde{V}$  corresponds to partially transposed state  $\hat{\rho}_{\chi G}$ . We can compute the logarithmic negativity of  $\hat{\rho}_{\chi G}$ , as shown in the last paragraph of the subsection 1.4.2, from the

symplectic eigenvalues  $\tilde{\nu}_k$  of the matrix  $\tilde{V}$ , the symplectic eigenvalues can be obtained from Eq.1.62. The logarithmic negativity computed in this way is marked as  $E_{\mathcal{N}_G}$ . The computation of  $E_{\mathcal{N}_G}$  can be done by hand analytically or numerically again with the help of the *QuTip*. Analytical calculation is not very exciting but it can be done from the definition of the covariance matrix  $V$  1.28. Occurring infinite sums from the infinite large Fock spaces used in the definition of the state are usually eliminated by Kronecker's deltas. Thus we can obtain exact (no dependence on the chosen size of dimensions)  $E_{\mathcal{N}_G}$ . The numerical approach is again limited by the dimension  $N'$  of Fock space. The state is defined in truncated Fock space and then the covariance matrix  $V(N')$  can be obtained, where the dependence on chosen  $N'$  is propagated. Therefore  $\tilde{\nu}_k(N')$  of the  $\tilde{V}(N')$  are also depended on  $N'$ , thus

$$E_{\mathcal{N}_G} \rightarrow E_{\mathcal{N}_G}(N'), \quad N' = \text{dim of trunc. Fock space.}$$

Before the discussion of a non-Gaussianity measure, we have to calibrate the used algorithms.

## 2.1 Calibration

In order to prevent any unnecessary errors, the first calculation is a calibration of the used algorithms. The best state for the calibration is the  $|\text{TMSV}\rangle$  itself. From Chapter 1, we know, that a two-mode squeezed vacuum may be obtained in a few ways. Firstly, we can use the two-mode squeezing operator on a two-mode vacuum  $|0, 0\rangle$ , 1.47. Secondly, we can also use two one-mode squeezing operators on one-mode vacua  $|0\rangle$ ,  $|0\rangle$ , 1.37. The one-mode squeezing operators have to squeeze each vacuum in the opposite way. Eventually, we use a balanced beam splitter and let the oppositely squeezed vacua interfere with that beam splitter, 1.41. To define these operators numerically, we have to again consider finite Hilbert space, thus in the *QuTip* we can define creation and annihilation operators in finite  $N$  dimensions, we had chosen a relatively small size of dimension

$$N = 15.$$

Later, we discuss that higher dimension is not calculable on an average laptop in a reasonable time. Therefore the resulting state  $|\text{TMSV}\rangle$  is dependent on  $N$  as well as its logarithmic negativity  $E_{\mathcal{N}_{NG}}(N)$ . In Figure 2.1 there is the logarithmic negativity relative to the squeezing parameter  $\lambda$ . The yellow curve corresponds to the two-mode squeezing operator and the orange curve corresponds to two one-mode squeezing plus the beam splitter operators.

We can also calculate  $E_{\mathcal{N}_G}$  of the  $|\text{TMSV}\rangle$  because it is a Gaussian state. The obtained exact form of  $\tilde{V}$  is

$$\tilde{V} = \begin{pmatrix} a & 0 & b & 0 \\ 0 & a & 0 & b \\ b & 0 & a & 0 \\ 0 & b & 0 & a \end{pmatrix},$$

where  $a$  and  $b$  are depended on  $\lambda$ . Thus symplectic eigenvalues are easily calculated as in Eq.1.62

$$\tilde{\nu}_{\pm} = (a \pm b),$$

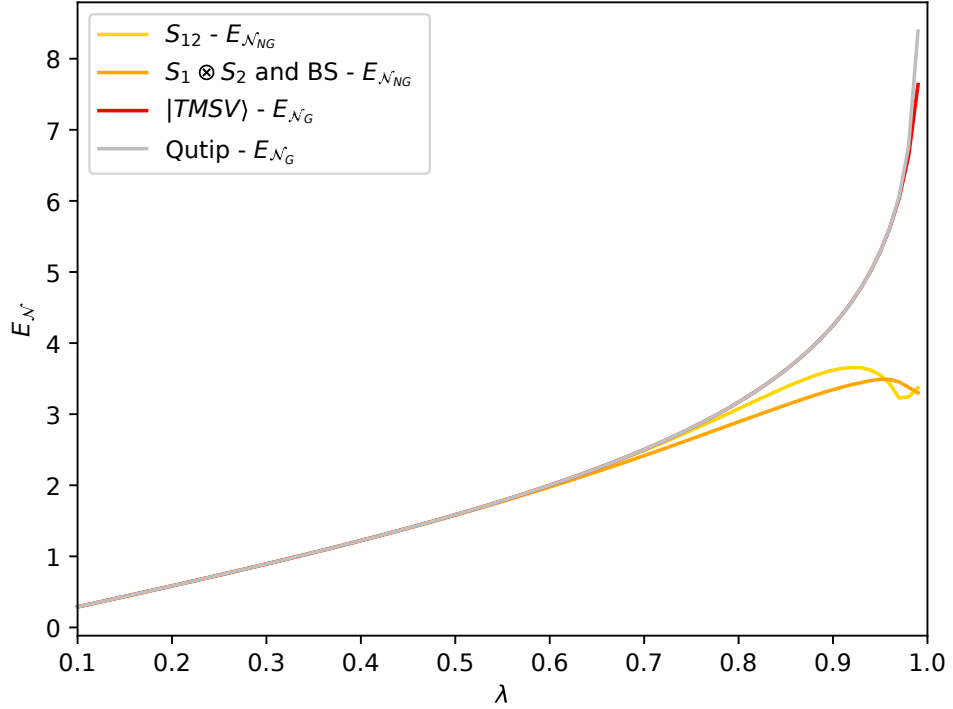


Figure 2.1: The logarithmic negativity relative to the squeezing parameter  $\lambda$ . The logarithmic negativity is  $E_{\mathcal{N}_{NG}}$  is computed for the  $|TMSV\rangle$  obtained from the two-mode squeezing operator it is represented by the yellow curve, the  $|TMSV\rangle$  obtained from the one-mode squeezing operators and the balanced beam splitter it is represented by the orange curve, both are calculated for the dimension  $N = 15$  of the Fock base. The Gaussian logarithmic negativity  $E_{\mathcal{N}_G}$  calculated analytically is represented by the red curve.  $E_{\mathcal{N}_G}$  computed numerically is the grey curve for the dimension of the Fock basis  $N' = 100$ .

with

$$a = \frac{1 + \lambda^2}{2(1 - \lambda^2)}, \quad b = \frac{2\lambda}{2(1 - \lambda^2)}.$$

And that is all we need to get  $E_{\mathcal{N}_G}$  of Eq.1.66. In Figure 2.1 the red curve is representing described approach.

As described in the introduction of the chapter, we can also compute  $E_{\mathcal{N}_G}$  numerically. We generate  $|\text{TMSV}\rangle$  directly from its definition in the Fock basis of Eq.2.1, then the  $E_{\mathcal{N}_G}$  is computed in dependence of the chosen size of dimension, it is really fast, we can set

$$N' = 100.$$

The grey curve is computed in this way in Figure 2.1. It uses inner functions of *QuTip*. For the  $\lambda \rightarrow 1$  it slightly deviates from the exact analytical approach (red). Thus the analytical solution and numerical solution of  $E_{\mathcal{N}_G}$  are interchangeable.

The state  $|\text{TMSV}\rangle$  is a Gaussian state, thus  $E_{\mathcal{N}_{NG}} = E_{\mathcal{N}_G}$ . For low squeezing (up to  $\lambda \approx 0.5$ ) we see an expected coverage of all curves. If we increased the dimension of Fock space  $N$ , we would get better coverage of the orange and yellow curves. Up to  $\lambda \approx 0.5$  it does not matter, which procedure we use for the computation of the logarithmic negativity of the  $|\text{TMSV}\rangle$ .

## 2.2 Subtraction of photon

In this section, we switch to the density operator formalism. We subtract a photon from  $\hat{\rho}_{\text{TMSV}}$  in order to create the non-Gaussian state  $\hat{\rho}$ .

How do we compute  $E_{\mathcal{N}_G}$  if the state is non-Gaussian? Despite that fact, we can 'Gaussify' the state. Let us explain. We can easily compute the covariance matrix  $V$  of the state  $\hat{\rho}$  as well as the Wigner function due to general Eq.1.20. We can also use this covariance matrix  $V$  and plug it into the Gaussian Wigner function Eq.1.27. We have obtained the Gaussian state  $\hat{\rho}_G$  described by the Gaussian Wigner function 1.27. So to one given covariance matrix, there exists two states: the non-Gaussian  $\hat{\rho}$  state and the Gaussian state  $\hat{\rho}_G$ . Please note that we do not need to know the specific form of  $\hat{\rho}_G$  because the logarithmic negativity  $E_{\mathcal{N}_G}$  is computed from the covariance matrix  $V$ , specifically from  $\tilde{V}$ . As already discussed it can be done by hand or numerically. If one decides to do it by hand, he or she will come to the general form of the covariance matrix

$$\tilde{V} = \begin{pmatrix} a_1 & 0 & c_1 & 0 \\ 0 & a_2 & 0 & c_2 \\ c_1 & 0 & b_1 & 0 \\ 0 & c_2 & 0 & b_2 \end{pmatrix}, \quad (2.6)$$

where all matrix elements are dependent on  $\lambda$ . There is no simple formula for symplectic eigenspectrum  $\tilde{\nu}_{\pm}$  as in the previous case. It is not interesting and useful to present it here. Numerical computation of  $E_{\mathcal{N}_G}$  gives roughly the same result as analytical like in the calibration section.

The logarithmic negativity  $E_{\mathcal{N}_{NG}}$  of  $\hat{\rho}$  can be computed numerically as previously.

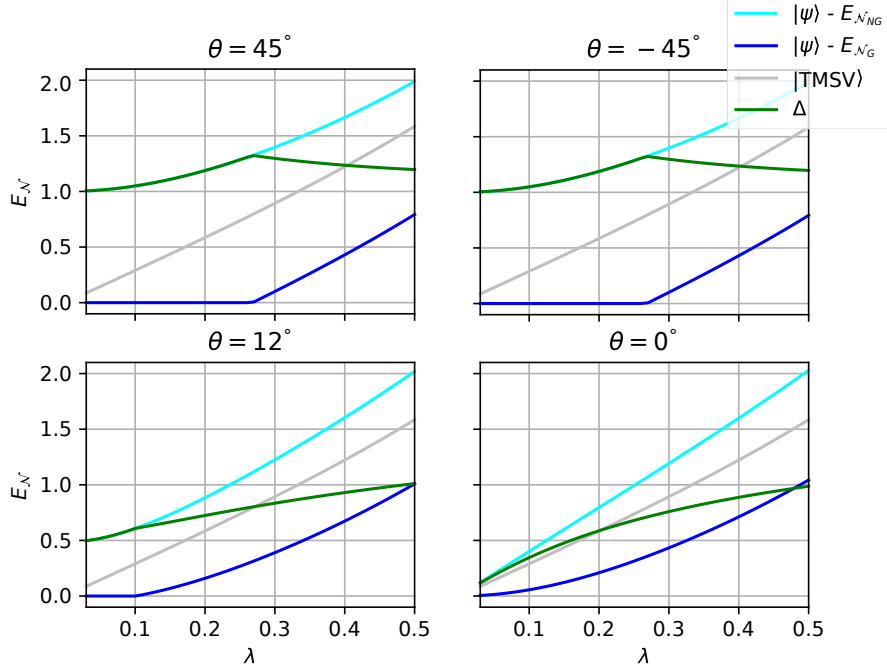


Figure 2.2: The logarithmic negativity relative to  $\lambda$ . The logarithmic negativity  $E_{\mathcal{N}_{NG}}$  computed for non-Gaussian state  $\hat{\rho}$  is represented by the cyan curve. The logarithmic negativity of the  $\hat{\rho}_{\text{TMSV}}$  computed in one chosen procedure is the grey curve. The logarithmic negativity  $E_{\mathcal{N}_G}$  of the Gaussified state  $\hat{\rho}_G$  is represented by the blue curve. The difference  $\Delta$  is the green curve.

In Figure 2.2 there are four plots, the parameter  $\theta$  is fixed for each plot and the parameter  $\lambda$  runs from 0 to 0.5. The grey curve corresponds to the logarithmic negativity of the  $\hat{\rho}_{\text{TMSV}}$  as before. The cyan curve corresponds to the logarithmic negativity  $E_{\mathcal{N}_{NG}}$  and the blue curve is the  $E_{\mathcal{N}_G}$ . We see that non-Gaussian entanglement always increases compared to the entanglement of the original two-mode squeezed state. The Gaussian entanglement always decreases. In some cases, it even goes to zero.

In the following, we always compute the difference  $\Delta$  of these two logarithmic negativities for a given non-Gaussian state and its Gaussified state.

$$\Delta = E_{\mathcal{N}_{NG}} - E_{\mathcal{N}_G}. \quad (2.7)$$

This difference should always be positive because the  $E_{\mathcal{N}_{NG}}$  contains full information about the state  $\hat{\rho}$  on the other hand Gaussified state does not contain the non-Gaussian part of the state so its logarithmic negativity  $E_{\mathcal{N}_G}$  should be lower. In principle, we have got how much of non-Gaussian entanglement is in the state  $\hat{\rho}$ , therefore the difference could be an indicator of the non-Gaussianity of the state. In Figure 2.2 the green curve is always the difference  $\Delta$  of the cyan and blue curves.

In Figure 2.3 there are shown the differences  $\Delta$  for various states with various fixed  $\theta$  to get different perspectives. We see that the balanced superposition  $\theta = 45^\circ$  of the state  $\hat{\rho}$  is always the highest.

If we want to interpret  $\Delta$  as a measure of non-Gaussianity, first of all, we have to define properties of non-Gaussianity:

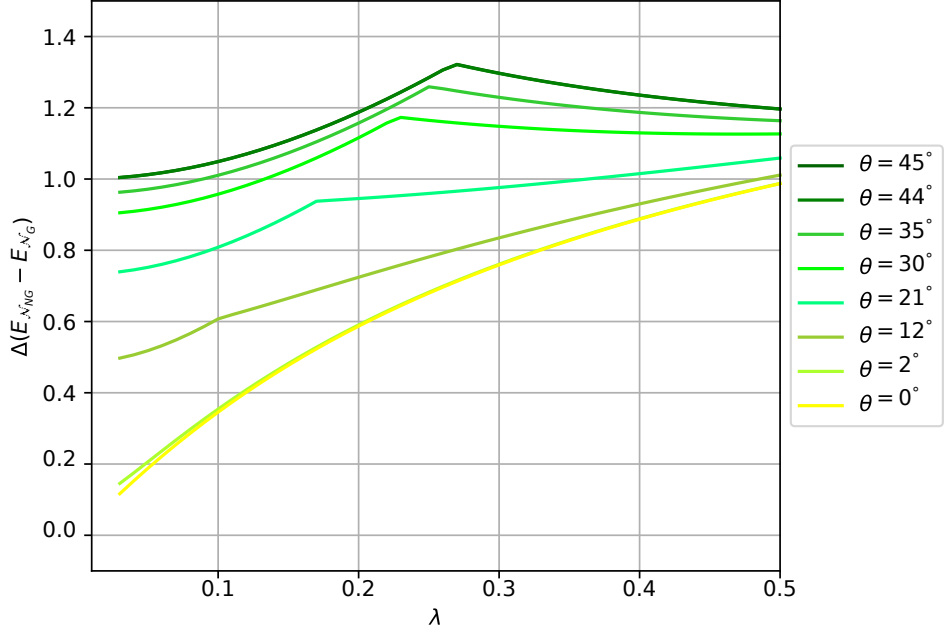


Figure 2.3: The difference  $\Delta$  of Gaussian and non-Gaussian entanglement relative to  $\lambda$ . The difference  $\Delta$  is always the highest for balanced superposition  $\theta = 45^\circ$ . The non-smooth point is connected with the non-smooth behavior of  $E_{NG}$ .

1. A non-Gaussianity is a functional from the set of quantum states to non-negative real numbers  $F : S(\mathcal{H}) \rightarrow \mathbb{R}^{0,+}$ .
2.  $F$  is zero for Gaussian states  $F(\hat{\rho}_G) = 0$ , where  $\hat{\rho}_G$  is a Gaussian state.
3. Monotonicity under deterministic Gaussian operations, for any Gaussian operation  $\Lambda_G$ , the functional must not increase  $F(\hat{\rho}) \geq F(\Lambda_G(\hat{\rho}))$ .

Some additional properties are usually convexity and additivity [8].

Firstly, obtained function  $\Delta$  is invariant under local Gaussian operations because the logarithmic negativity should not change under local operations (one-mode squeezers) [14]. However, non-local Gaussian operations (beam splitter) can change the  $\Delta$ , it can be seen in the next section, thus the third condition is not satisfied.

Secondly, as you can see from the plots 2.2, it does not meet the second condition for all  $\lambda$ . Thus we should look for a better (in terms of axioms) measure of non-Gaussianity.

### 2.2.1 Looking for measure

In the following, we will use a series of Gaussian unitaries  $U_S$  acting on the state  $|\psi\rangle$  to adjust  $\Delta$  in order to meet the axioms of the non-Gaussianity. We can adjust the covariance matrix  $V$  of the non-Gaussian state  $\hat{\rho}$ . The Williamson form of Eq.1.59 transforms  $V$  to its symplectic diagonal form  $V^\oplus$ . From the discussion in the Bloch-Messiah section 1.5, we know that  $V^\oplus$  corresponds to the

tensor product of two thermal states of Eq.1.68. Thus the Gaussian logarithmic negativity

$$E_{\mathcal{N}_G} \rightarrow 0$$

should go to zero because the tensor product of two sub-systems is equivalent to a separable state of the whole system. This modifies our measure to just

$$\Delta = E_{\mathcal{N}_{NG}}. \quad (2.8)$$

So our procedure is following, we have to find  $S$  that symplectically diagonalizes the covariance matrix  $V$ , then find the corresponding Gaussian unitary  $U_S$ , and eventually, we use this unitary to non-Gaussian state  $|\psi\rangle$ ,  $U_S|\psi\rangle$ . The covariance matrix  $V^\oplus$  of the state  $U_S|\psi\rangle$  gives  $E_{\mathcal{N}_G} = 0$  and non-zero  $E_{\mathcal{N}_G}$ .

For the procedure described above, we use a slightly different form of the Williamson decomposition than used in Eq.1.59

$$V^\oplus = SVS^T.$$

We remind you, that we are able to find the symplectic eigenspectrum from the Eq.1.62, so our problem reduces to find  $S$  from known  $V$  and  $V^\oplus$ . Here comes the Bloch-Messiah decomposition of Eq.1.70, we directly plug the decomposition of  $S$  into the Williamson form

$$V^\oplus = S_{B2} \left[ \bigoplus_{k=1}^2 S_{Sq}(r_k) \right] S_{B1} V S_{B1}^T \left[ \bigoplus_{k=1}^2 S_{Sq}(r_k) \right] S_{B2}^T.$$

From the Eq.1.40 we know the form of  $S_{Bi}$  and from the Eq.1.38 we know  $S_{Sq}$ . This matrix equation has six variables  $(t_1, t_2, v_1, v_2, r_1, r_2)$ , but just four of them are independent due to conditions

$$t_1^2 + v_1^2 = 1, \quad t_2^2 + v_2^2 = 1.$$

One of the tricks, how to simplify the system of these non-linear equations is re-arrangement of the system in the following way:

$$S_{B2}^T V^\oplus S_{B2} = \left[ \bigoplus_{k=1}^2 S_{Sq}(r_k) \right] S_{B1} V S_{B1}^T \left[ \bigoplus_{k=1}^2 S_{Sq}(r_k) \right]. \quad (2.9)$$

Another trick consists of the transformation of the covariance matrix  $V$  of Eq.2.6.<sup>1</sup> Basically, it is just a form change of the covariance matrix under local Gaussian operations. The proof can be found in [34], the new form of the covariance matrix is

$$V' \leftrightarrow \left[ \bigoplus_{k=1}^2 S_{Sq}(r'_k) \right] V \left[ \bigoplus_{k=1}^2 S_{Sq}(r'_k) \right] \quad (2.10)$$

where  $V'$  is simplified as follows

$$V' = \begin{pmatrix} m & 0 & c_+ & 0 \\ 0 & m & 0 & c_- \\ c_+ & 0 & n & 0 \\ 0 & c_- & 0 & n \end{pmatrix}$$

---

<sup>1</sup>We remind you, there is a simple relation between  $V$  and  $\tilde{V}$ , see 1.57.



Matrix elements can be obtained from the elements of the covariance  $V$

$$\begin{aligned} m &= \sqrt{a_1 a_2}, & n &= \sqrt{b_1 b_2}, \\ c_+ &= c_1 \sqrt[4]{\frac{a_2 b_2}{a_1 b_1}}, & c_- &= c_2 \sqrt[4]{\frac{a_1 b_1}{a_2 b_2}}. \end{aligned}$$

It is usually called the standard form of the covariance matrix. Therefore Eq.2.9 is

$$S_{B2}^T V^\oplus S_{B2} = \left[ \bigoplus_{k=1}^2 S_{S_q}(r_k) \right] S_{B1} V' S_{B1}^T \left[ \bigoplus_{k=1}^2 S_{S_q}(r_k) \right]. \quad (2.11)$$

After some time spent playing with the system of Eq.2.11, we are able to find an equation that depends only on one of the four unknown variables,  $t_2$ , this equation is the order of eight with square roots

$$\alpha_1 \alpha_2 \beta_1 \beta_2 - (\nu_+ \nu_- + \gamma_1 \gamma_2)^2 = 0,$$

where

$$\begin{aligned} \alpha_1 &= m + 2c_+ t_2 \sqrt{1 - t_2^2}, \\ \alpha_2 &= m + 2c_- t_2 \sqrt{1 - t_2^2}, \\ \beta_1 &= m - 2c_+ t_2 \sqrt{1 - t_2^2}, \\ \beta_2 &= m - 2c_- t_2 \sqrt{1 - t_2^2}, \\ \gamma_1 &= c_+ (2t_2^2 - 1), \\ \gamma_2 &= c_- (2t_2^2 - 1). \end{aligned}$$

Probably it is not possible to find an analytical solution. We have used a numerical solver implemented in *Python* library - *Scipy*. Solutions for remaining variables can be found analytically. Now with solved variables at hand, we can find the corresponding Gaussian unitaries  $U_{S_q}(r_{1,2}), U_{B1}, U_{B2}$  from Eq.1.41 and Eq.1.37. We should not forget about transformation into the standard form in Eq.2.10, we have to also implement  $U_{S_q}(r'_{1,2})$ . Therefore, we can write the Bloch-Messiah decomposition of  $U_S$

$$U_S = U_{B2} \left[ \bigotimes_{k=1}^2 U_{S_q}(r_k) \right] U_{B1} \left[ \bigotimes_{k=1}^2 U_{S_q}(r'_k) \right]$$

For given  $\theta$ , we are able to plot  $E_{\mathcal{N}_G}$  of the state  $U_S|\psi\rangle$  relative to  $\lambda$ , it is the green curve in Figure 2.4. There is also  $E_{\mathcal{N}_G}$ , the blue curve, which is a control curve of the algorithm of computation of  $U_S$ , we can see, that it is always zero, thus our algorithm works fine. Figure 2.5 compares differences  $\Delta$  for more  $\theta$ .

Comparing Figures 2.3 and 2.5 there is an interesting result, in the case of  $\theta = 45^\circ$ . It goes from maximum  $\Delta$  in the first Figure to minimum  $\Delta$  in the second for all  $\lambda$ . But why? The  $\hat{\rho}_{\text{TMSV}}$  state from which  $\hat{\rho}$  originates is generated via two one-mode squeezers and one beam splitter operation. After the action of  $U_S$ , which consists of two beam splitters and two one-mode squeezers, the state  $U_S$  is completely disentangled, one of the beam splitters is balanced and the other

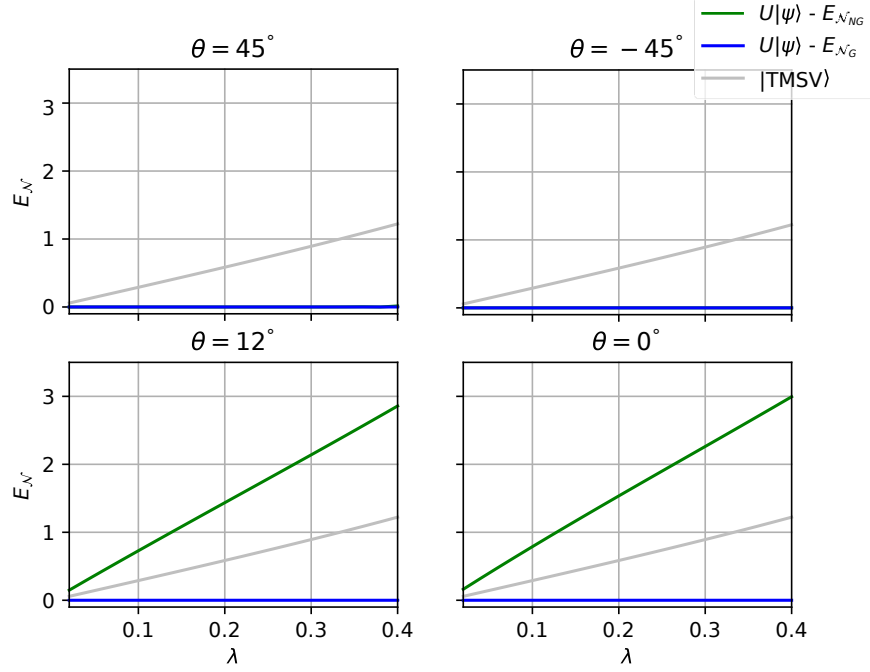


Figure 2.4: The logarithmic negativity relative to  $\lambda$ . The logarithmic negativity  $E_{\mathcal{N}_{NG}}$  computed for non-Gaussian state  $U_S \hat{\rho} U_S^\dagger$  is represented by the green curve. The logarithmic negativity of the  $\hat{\rho}_{\text{TMSV}}$  computed in one chosen procedure is the grey curve. The logarithmic negativity  $E_{\mathcal{N}_G}$  of the Gaussified stat  $U_S \hat{\rho}_G U_S^\dagger$  is the blue curve.

has a transmissivity coefficient equal to one. Ideal beam splitters are reversible devices.

Let us discuss the properties of the new  $\Delta$ . The potential measure of non-Gaussianity  $\Delta$  of the state  $U_S |\psi\rangle$  definitely fulfills the first condition, the logarithmic negativity  $E_{\mathcal{N}_{NG}}$  is always positive it can be seen from the definition. The second condition is also fulfilled because for Gaussian states hold  $E_{\mathcal{N}_{NG}} = E_{\mathcal{N}_G} = 0$ . The third condition - monotonicity: If we use a Gaussian unitary  $U_G \equiv U_B, U_{Sq}$  on a given state  $|\psi\rangle$

$$|\phi\rangle \equiv U_G |\psi\rangle,$$

we can use the procedure above, but instead of looking for  $U_S$ , we have to look for  $U_{S'}$  which corresponds to  $S'$ . This  $S'$  symplectically diagonalizes the covariance matrix of the state  $|\phi\rangle$ . With that procedure the Gaussian logarithmic negativity  $E_{\mathcal{N}_G}$  is always zero. What about  $E_{\mathcal{N}_{NG}}$ ? Figure 2.6 is the same plot as the plot in the left bottom corner in Figure 2.4. The green curve is the same non-Gaussian logarithmic negativity of the state  $U_S |\psi\rangle$  and the non-Gaussian logarithmic negativities of the state  $U_{S'} |\phi\rangle$  are the red and the orange curves. We have tried random Gaussian unitaries, the red corresponds to  $U_G = U_B(\theta = \pi/6)$  and the orange one is  $U_G = U_{Sq}(r_1 = 0.2)$ . They both cover the green. Thus we have numerically shown that  $\Delta = E_{\mathcal{N}_{NG}}$  is invariant under Gaussian operations. The  $U_{S'}$  always compensates for  $U_G$  because  $U_{S'}$  is a series of Gaussian operations. Therefore, the third condition is also fulfilled.

Given any non-Gaussian state, we can find a corresponding Gaussified state. To find the thermal decomposition 1.67 of the Gaussified state, we have to solve

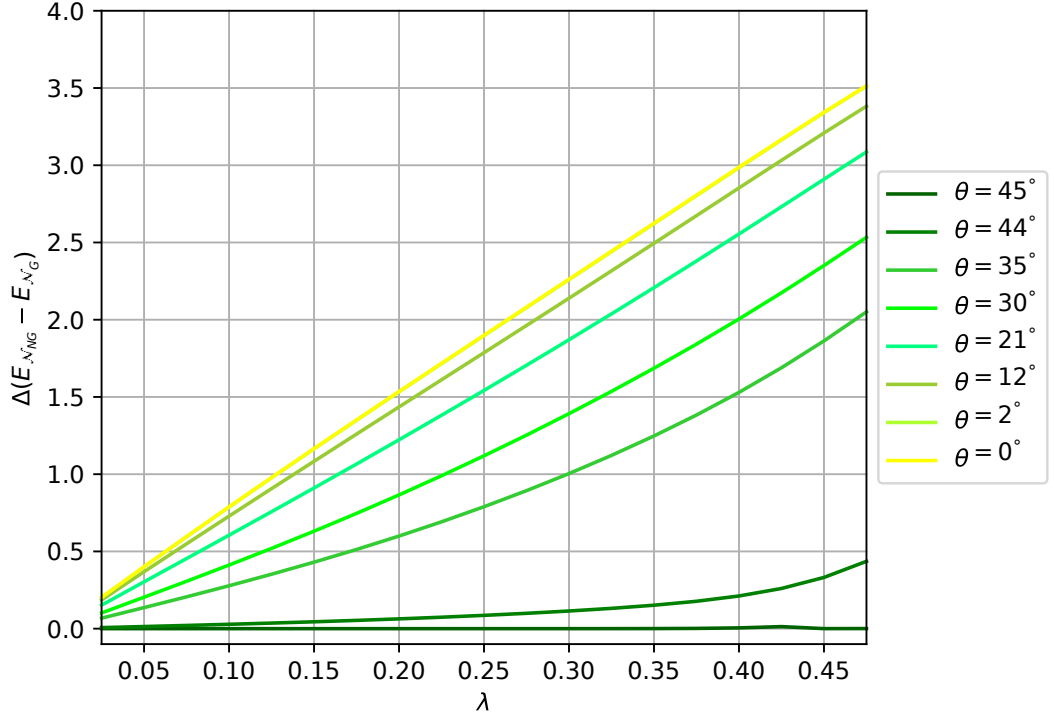


Figure 2.5: The difference  $\Delta$  relative to  $\lambda$ . The difference  $\Delta$  is the lowest for balanced superposition  $\theta = 45^\circ$ .

the Williamson decomposition 1.59 with the help of Bloch-Messiah decomposition 1.69. If we know the unitary operator occurring in thermal decomposition, we act with it on a non-Gaussian state, then its Gaussified state is a separable state of one-mode thermal states 1.68, thus Gaussian entanglement is zero and the non-Gaussian entanglement is invariant under Gaussian operations. Any Gaussian operation is compensated by Gaussian operations in the Bloch-Messiah decomposition. Therefore, with this procedure at hand, the  $\Delta$  fulfills all axioms of the non-Gaussianity measure.

We should comment on why the entropy of entanglement was not used even if the two-mode squeezed state  $\hat{\rho}_{\text{TMSV}}$  and non-Gaussian state  $\hat{\rho}$  are both pure states. The measure based on the difference of entropies of a non-Gaussian state and its Gaussified state would not look like the difference of logarithmic negativities because Gaussian states are the states with the highest entropy [39]. The entropy is invariant under unitary transformations and thanks to the Williamson decomposition 1.59 every Gaussian state can be decomposed to the tensor product of thermal states 1.68 and thermal states maximize the entropy. This property can be used to define non-Gaussianity measure in the case of one-mode Gaussian states because there is no entanglement [8]. It measures the distance between the non-Gaussian states from the Gaussian ones in terms of entropy. In the case of bipartite states, the entropy starts to measure also the entanglement of the system. Thus it would not be clear, what the difference between non-Gaussian entropy and Gaussian entropy would mean. The second reason is that we do not know the form of the Gaussified state  $\hat{\rho}_G$ , it can be also the mixed state.

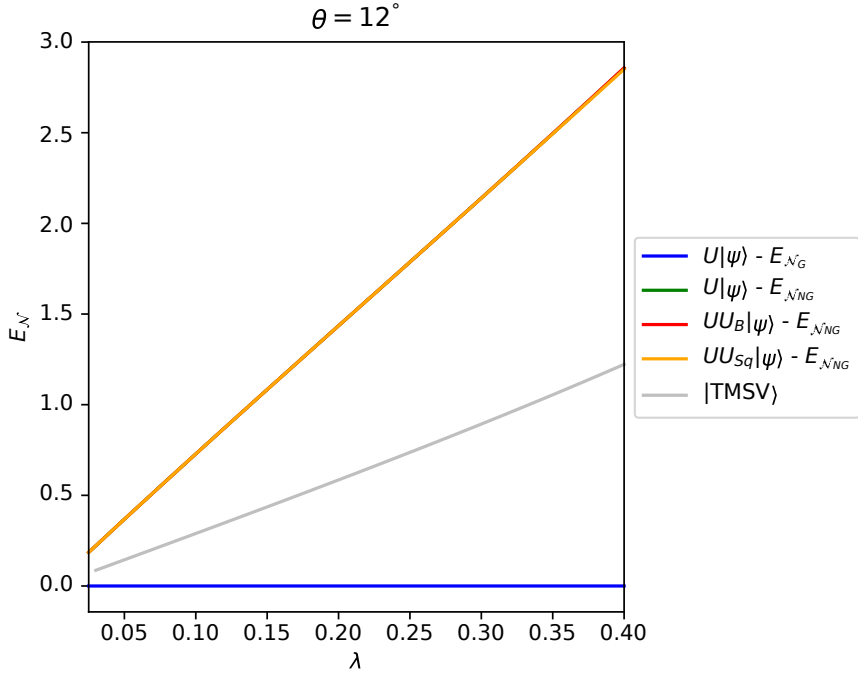


Figure 2.6: The logarithmic negativity relative to  $\lambda$ . It is the same plot as the plot in the left-bottom corner in Figure 2.4. It is the numerical proof of the invariance of the  $\Delta$  under Gaussian operations. The red curve corresponds to  $U_G = U_B(\theta = \pi/6)$ , the orange to  $U_G = U_{Sq}(r_1 = 0.2)$ .

## 2.3 Comparing to other measures

### 2.3.1 Wigner negativity

Going back to Figure 2.5, one may ask, if there is another measure of non-Gaussianity to find the interpretation of  $\Delta$ . As discussed in the section 1.7, there is a measure of non-Gaussianity based on the Wigner negativity. Therefore, we need to compute the Wigner function of a given non-Gaussian state. It turned out, there is no algorithm for a calculation of the Wigner function in two modes. We have taken the algorithm for computation of the Wigner function in one mode in *QuTip* and we have tried to extend it to two modes. The original iterative method is based on the definition of the Wigner function 1.22

$$W = \sum_{nm} \rho_{nm} \tilde{W}_{nm}(x, p),$$

where  $\rho_{nm}$  is the matrix element of the density matrix  $\hat{\rho}$

$$\hat{\rho} = \sum_{nm} \rho_{nm} |n\rangle \langle m|$$

of a given state. Therefore  $\tilde{W}_{nm}$  is the Wigner function of an element  $n, m$ . Due to the integral relation between Hermite and Laguerre polynomials [40], we can express

$$\tilde{W}_{nm} = \frac{(-1)^m}{\pi} \sqrt{\frac{m!}{n!}} \left( \sqrt{2}(x + ip) \right)^{n-m} e^{-(x^2+p^2)} L_m^{(n-m)} \left( 2(x^2 + p^2) \right),$$

where  $L_n^{(\alpha)}(y)$  is the associated  $n$ -th Laguerre polynomial. The algorithm itself is based on the recurrence relation for the Laguerre polynomials. Our extension consists of the addition of a second mode

$$W = \sum_{n_1 m_1 n_2 m_2} \rho_{n_1 m_1 n_2 m_2} \tilde{W}_{n_1 m_1}(x_1, p_1) \tilde{W}_{n_2 m_2}(x_2, p_2).$$

After some time of calibration, we have partly succeeded because the algorithm is really slow due to the product of two Laguerre polynomials. We are able to compute the Wigner function in two modes.

We can use our algorithm to compute squeezed Wigner function of the  $U_S|\psi\rangle$ . Obviously, we are not able to show the whole four-dimensional Wigner space, we have to choose which variables  $(x_1, p_1, x_2, p_2)$  we set to zero or to any other value. It is a sort of cut of that space. In Figure 2.7 we chose one state with  $\lambda = 0.1$  and  $\theta = 45^\circ$ , we set  $p_1 = p_2 = 0$ . It has some Wigner negativity (at this stage it is not important to quantify the Wigner negativity).

Compared with Figure 2.5 the state  $U_S|\psi\rangle$  for  $\theta = 45^\circ$  should be Gaussian because  $\Delta = 0$  but in Figure 2.7, you can clearly see, that the state for  $\lambda = 0.1$  and  $\theta = 45^\circ$  is non-Gaussian. Even if the Figure shows only cut in the whole Wigner space. Therefore the measure of non-Gaussianity  $\Delta$  does not measure the non-Gaussianity based on the state's negativity in the Wigner representation. Nevertheless, the non-Gaussian states are not the only states with a negative Wigner function. It remains open, to what a property of the non-Gaussian states  $\Delta$  measures.

The possible interpretation can be the following: From Figure 2.5 we see that  $\Delta$  is always the highest for  $\theta = 0^\circ$ , this corresponds to subtraction only in one mode. So this state is created by the local non-Gaussian operation. We also see that  $\Delta$  is always the lowest for  $\theta = 45^\circ$ , this corresponds to balanced subtraction from both modes. So this state is created by non-local non-Gaussian operation. Therefore  $\Delta$  is not able to detect non-Gaussianity which was obtained by non-local non-Gaussian operations. So even if the states with  $\theta = 45^\circ$  are non-Gaussian  $\Delta$  vanishes.

In the next research, we should test more states, with multi-photon subtraction or photon addition. Also, the algorithm for the computation of the Wigner function of multi-mode states should be optimized because we lacked computation power during computations of highly squeezed states, high squeezing demanded a higher size of the Fock basis.

$U_S|\psi\rangle, \lambda = 0.1, \theta = 45^\circ$

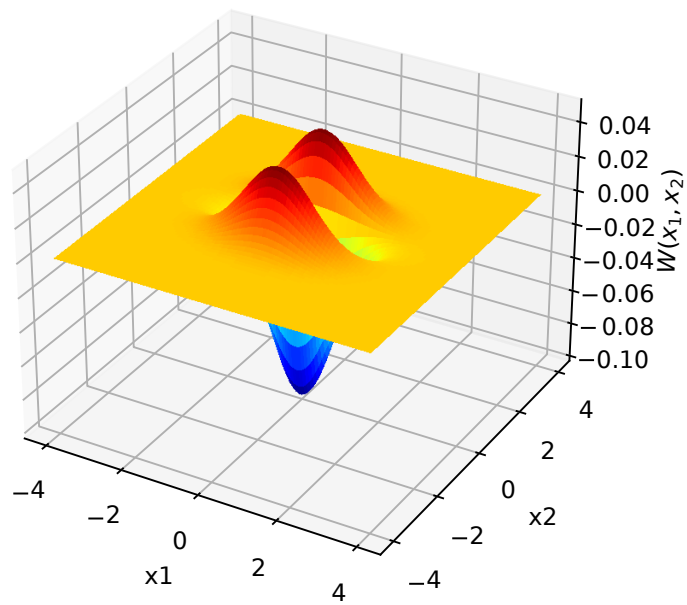


Figure 2.7: The Wigner function  $W(x_1, 0, x_2, 0)$  of the state  $U_S|\psi\rangle$  with  $\lambda = 0.1$  and  $\theta = 45^\circ$ .

# Conclusion

We have found the procedure how to find the measure of non-Gaussianity  $\Delta$  for two-mode bipartite systems. It is based on the difference between non-Gaussian and Gaussian entanglement of the state. With the usage of Gaussian unitaries, we were able to vanish the Gaussian entanglement and the remaining non-Gaussian entanglement meets the axioms of non-Gaussianity measure. However, it is not clear what property of non-Gaussian states it measures. During the search for an interpretation of the non-Gaussianity measure  $\Delta$ , we have extended the numerical algorithm for the computation of the Wigner function to two modes.

In future research, other two-mode Gaussian states should be tested, e.g. multi-photon subtracted states or states with added photons. Based on the results the property of non-Gaussian states which is measured by  $\Delta$  should be revealed. If the interpretation is found, the research can have a significant impact in the field of non-Gaussian states because it would give a new perspective on how to look at non-Gaussian states. The understanding of non-Gaussian states implies progress in the field of quantum computing.

# Bibliography

- [1] de Leon, N. P., et al., *Materials challenges and opportunities for quantum computing hardware*, Science, 372, 6539, 2021
- [2] Braunstein, S. L., van Loock, P., *Quantum information with continuous variables*, Review of Modern Physics, 77, 513, 2005
- [3] Flamini, F., Sapgno, N., Sciarrino, F., *Photonic quantum information processing: a review*, Reports on Progress in Physics, 82, 016001, 2019
- [4] Weedbrook, Ch., et al., *Gaussian quantum information*, Review of Modern Physics, 84, 621, 2012
- [5] Bartlett, S. D., Sanders, B. C., Braunstein, S. L., Nemoto, K. *Efficient Classical Simulation of Continuous Variable Quantum Information Processes*, Physical Review Letters, 88, 097904, 2002
- [6] Lloyd, S., Braunstein, S. L., *Quantum Computation over Continuous Variables*, Physical Review Letters, 82, 1784, 1999
- [7] Mari, A., Eisert, J., *Positive Wigner functions render classical simulation of quantum computation efficient*, Physical Review Letters, 109, 230530, 2012
- [8] Albarelli, F., Genoni, M. G., Paris, M. G. A., Ferraro, A. *Resource theory of quantum non-Gaussianity and Wigner negativity*, Physical Review A, 98, 052350, 2018
- [9] Tan, K. Ch., Choi, S., Jeong, H., *Negativity of quasiprobability distributions as a measure of nonclassicality*, Physical Review Letters, 124, 110404, 2020
- [10] Walschaers, M., *Non-Gaussian quantum states and where to find them*, Physical Review X, 2, 030204, 2021
- [11] Horodecki, R., Horodecki, P., Horodecki, M., Horodecki, K., *Quantum Entanglement*, Review of Modern Physics, 81, 865, 2009
- [12] Peres, A., *Separability Criterion for Density Matrices*, Physical Review Letters, 77, 1413, 1996
- [13] Horodecki, M., Horodecki, P., Horodecki, R., *Separability of mixed states: necessary and sufficient conditions*, Physical Letters A, 223, 1, 1996
- [14] Vidal, G., Werner, R. F., *Computable measure of entanglement*, Physical Review A, 65, 032314, 2002
- [15] Heidmann, A., et al., *Observation of Quantum Noise Reduction on Twin Laser Beams*, Physical Review Letters, 59, 2555, 1987
- [16] Takahashi, H., et al., *Entanglement distillation from Gaussian input states*, Nature Photonics, 4, 178, 2010



- [17] Mamoru E., et al., *Non-Gaussian quantum state generation by multi-photon subtraction at the telecommunication wavelength*, Optics Express, 31, 12865, 2023
- [18] Leonhardt, U., *Essential Quantum Optics, From Quantum Measurements to Black Holes*, Cambridge University Press, ISBN 978-0-521-86978-2, 2010
- [19] Cejnar, P., *A Condensed Course of Quantum Mechanics*, Karolinum Press, ISBN 978-80-246-2349-8, 2013
- [20] Simon, R., Mukunda, N., Dutta, B., *Quantum noise matrix for multimode systems:  $U(n)$  invariance, squeezing, and normal forms*, Physical Review A, 49, 1567, 1994
- [21] Hudson, R. L., *When is the Wigner quasi-probability density non-negative?*, Reports on Mathematical Physics, 6, 249, 1974
- [22] Slusher, R., et al., *Observation of squeezed states generated by four-wave mixing in an optical cavity*, Physical Review Letters, 55, 2409, 1985
- [23] Walls, D. F., Milburn, G. J., *Quantum optics 2ed.*, Springer, ISBN 978-3-540-28573-1, 2008
- [24] Einstein, A., Podolsky, B., and Rosen, N., *Can quantum-mechanical description of physical reality be considered complete?*, Physical Review, 47, 777, 1935
- [25] Schrödinger, E., *Discussion of Probability Relations between Separated Systems*, Mathematical Proceedings of the Cambridge Philosophical Society, 31, 555, 1935
- [26] Reid, M. D., *Demonstration of the Einstein-Podolsky-Rosen paradox using nondegenerate parametric amplification*, Physical Review A, 40, 913, 1989
- [27] Furusawa, A., et al., *Unconditional Quantum Teleportation*, Science, 282, 706, 1998
- [28] Ou, Z. Y., Mandel, L., *Violation of Bell's Inequality and Classical Probability in a Two-Photon Correlation Experiment*, Physical Review Letters, 61, 50, 1988
- [29] Lvovsky, A. I., *Quantum State Reconstruction of the Single-Photon Fock State*, Physical Review Letters, 87, 050402, 2001
- [30] Simon, R., *Peres-Horodecki Separability Criterion for Continuous Variable Systems*, Physical Review Letters, 84, 2726, 2000
- [31] Williamson, J., *On the Algebraic Problem Concerning the Normal Forms of Linear Dynamical Systems*, American Journal of Mathematics, 58, 141, 1936
- [32] Serafini, A., Illuminati, F., De Siena, S., *Symplectic invariants, entropic measures and correlations of Gaussian state*, Journal of Physics B, 37, L21, 2004

- [33] Pirandola, S., Serafini, A., Lloyd, S., *Correlation matrices of two-mode bosonic systems*, Physical Review A, 79, 052327, 2009
- [34] Duan, L. M., Giedke, G., Cirac, J. I., Zoller, P., *Inseparability criterion for continuous variable systems*, Physical Review Letters, 84, 2722, 2000
- [35] Braunstein, S. L., *Squeezing as an irreducible resource*, Physical Review A, 71, 055801, 2005
- [36] Zavatta, A., Parigi, V., Kim, M. S., Bellini, M., *Subtracting photons from arbitrary light fields: experimental test of coherent state invariance by single-photon annihilation*, New Journal of Physics, 10, 123006, 2008
- [37] Kenfack, A., Życzkowski, K., *Negativity of the Wigner function as an indicator of non-classicality*, Journal of Optics B, 6, 396, 2004
- [38] Johansson, J. R., Nation, P. D., Nori, F., *QuTiP 2: A Python framework for the dynamics of open quantum systems*, Computer Physics Communications, 184, 1234, 2013
- [39] Holevo, A. S., Sushma, M., Hirota, O., *Capacity of quantum gaussian channels*, Physical Review A, 59, 1820, 1999
- [40] Schleich, P. W., *Quantum optics in phase space*, Wiley-VCH, ISBN 3-527-29435-X, 2001

# List of Figures

1.1	Bloch-Messiah decomposition . . . . .	19
2.1	The logarithmic negativity relative to the squeezing parameter $\lambda$ . The logarithmic negativity is $E_{\mathcal{N}_{NG}}$ is computed for the $ \text{TMSV}\rangle$ obtained from the two-mode squeezing operator it is represented by the yellow curve, the $ \text{TMSV}\rangle$ obtained from the one-mode squeezing operators and the balanced beam splitter it is represented by the orange curve, both are calculated for the dimension $N = 15$ of the Fock base. The Gaussian logarithmic negativity $E_{\mathcal{N}_G}$ calculated analytically is represented by the red curve. $E_{\mathcal{N}_G}$ computed numerically is the grey curve for the dimension of the Fock basis $N' = 100$ . . . . .	24
2.2	The logarithmic negativity relative to $\lambda$ . The logarithmic negativity $E_{\mathcal{N}_{NG}}$ computed for non-Gaussian state $\hat{\rho}$ is represented by the cyan curve. The logarithmic negativity of the $\hat{\rho}_{\text{TMSV}}$ computed in one chosen procedure is the grey curve. The logarithmic negativity $E_{\mathcal{N}_G}$ of the Gaussified state $\hat{\rho}_G$ is represented by the blue curve. The difference $\Delta$ is the green curve. . . . .	26
2.3	The difference $\Delta$ of Gaussian and non-Gaussian entanglement relative to $\lambda$ . The difference $\Delta$ is always the highest for balanced superposition $\theta = 45^\circ$ . The non-smooth point is connected with the non-smooth behavior of $E_{\mathcal{N}_G}$ . . . . .	27
2.4	The logarithmic negativity relative to $\lambda$ . The logarithmic negativity $E_{\mathcal{N}_{NG}}$ computed for non-Gaussian state $U_S \hat{\rho} U_S^\dagger$ is represented by the green curve. The logarithmic negativity of the $\hat{\rho}_{\text{TMSV}}$ computed in one chosen procedure is the grey curve. The logarithmic negativity $E_{\mathcal{N}_G}$ of the Gaussified stat $U_S \hat{\rho}_G U_S^\dagger$ is the blue curve. . . . .	30
2.5	The difference $\Delta$ relative to $\lambda$ . The difference $\Delta$ is the lowest for balanced superposition $\theta = 45^\circ$ . . . . .	31
2.6	The logarithmic negativity relative to $\lambda$ . It is the same plot as the plot in the left-bottom corner in Figure 2.4. It is the numerical proof of the invariance of the $\Delta$ under Gaussian operations. The red curve corresponds to $U_G = U_B(\theta = \pi/6)$ , the orange to $U_G = U_{Sq}(r_1 = 0.2)$ . . . . .	32
2.7	The Wigner function $W(x_1, 0, x_2, 0)$ of the state $U_S \psi\rangle$ with $\lambda = 0.1$ and $\theta = 45^\circ$ . . . . .	34

# List of Abbreviations

CV... continuous variables

TMSV... two-mode squeezed vacuum

EPR... Einstein, Podolsky, Rosen

PPT... positive partial transpose criterion

LOCC... local operations and classical communication

WLN... Wigner logarithmic negativity